Computers in Biology and Medicine 149 (2022) 106073

Contents lists available at ScienceDirect

Computers in Biology and Medicine

journal homepage: www.elsevier.com/locate/compbiomed

# Breast cancer detection using deep learning: Datasets, methods, and challenges ahead

Nusrat Mohi ud din [a,*], Rayees Ahmad Dar [a], Muzafar Rasool [b], Assif Assad [a]

[a] Department of Computer Science and Engineering, Islamic University of Science and Techonology Kashmir, Awantipora, 192122, J&K, India
[b] Department of Computer Science, Islamic University of Science and Techonology Kashmir, Awantipora, 192122, J&K, India

ARTICLE INFO

*Keywords:*
Breast Cancer
Convolution neural networks
Deep learning
Mammography
Histopathology
MRI
Ultrasound
Thermography

ABSTRACT

Breast Cancer (BC) is the most commonly diagnosed cancer and second leading cause of mortality among women. About 1 in 8 US women (about 13%) will develop invasive BC throughout their lifetime. Early detection of this life-threatening disease not only increases the survival rate but also reduces the treatment cost. Fortunately, advancements in radiographic imaging like "Mammograms", "Computed Tomography (CT)", "Magnetic Resonance Imaging (MRI)", "3D Mammography", and "Histopathological Imaging (HI)" have made it feasible to diagnose this life-taking disease at an early stage. However, the analysis of radiographic images and Histopathological images is done by experienced radiologists and pathologists, respectively. The process is not only costly but also error-prone. Over the last ten years, Computer Vision and Machine Learning (ML) have transformed the world in every way possible. Deep learning (DL), a subfield of ML has shown outstanding results in a variety of fields, particularly in the biomedical industry, because of its ability to handle large amounts of data. DL techniques automatically extract the features by analyzing the high dimensional and correlated data efficiently. The potential and ability of DL models have also been utilized and evaluated in the identification and prognosis of BC, utilizing radiographic and Histopathological images, and have performed admirably. However, AI has shown good claims in retrospective studies only. External validations are needed for translating these cutting-edge AI tools as a clinical decision maker. The main aim of this research work is to present the critical analysis of the research and findings already done to detect and classify BC using various imaging modalities including "Mammography", "Histopathology", "Ultrasound", "PET/CT", "MRI", and "Thermography". At first, a detailed review of the past research papers using Machine Learning, Deep Learning and Deep Reinforcement Learning for BC classification and detection is carried out. We also review the publicly available datasets for the above-mentioned imaging modalities to make future research more accessible. Finally, a critical discussion section has been included to elaborate open research difficulties and prospects for future study in this emerging area, demonstrating the limitations of Deep Learning approaches.

## 1. Introduction

According to the "International Agency for Research on Cancer (IARC's) 2020 World Cancer Report", Cancer is the primary or secondary cause of deathblow (ages 30–69) in 134 out of 183 countries (see Fig. 1). Lung cancer is by far the leading cause of death among men and women, but in men prostate cancer is more common and in women BC is more common. As reported by IARC, cancer incidence is anticipated to inflate from 18.1 million to 29.5 million between 2018 and 2040, with mortality rising from 9.6 million to 16.4 million. Of all types of cancers, BC is one of the most colloquial and deadliest cancers among women. BC is the most prevalent cancer with high mortality and morbidity among women in the world and constitutes about 14% of all cancers[1] as shown in Fig. 2. It increases the death rate among women, affecting about 2.1 million women each year. It is estimated that 6,85,000 women died due to BC in 2020. Death rates in wealthy countries are significantly higher, and they are rising in every region of the world. Cancer is the abnormal cell division due to which a mass is developed called a tumor. The tumor can be cancerous (malignant) or non-cancerous (Benign). Breast Cancer is the malignant tumor that develops from breast cells. BC usually begins in the cells of the lobules, which are the milk producing ducts, the passage that drain milk from the lobules to the nipple. over time,

* Corresponding author.
*E-mail addresses:* nusrat.mohiuddin@islamicuniversity.edu.in (N.M.u. din), darrayees@gmail.com (R.A. Dar), muzafar.rasool@islamicuniversity.edu.in (M. Rasool), assif.assad@islamicuniversity.edu.in (A. Assad).

[1] http://cancerindia.org.in/globocan-2018-india-factsheet.

https://doi.org/10.1016/j.compbiomed.2022.106073
Received 22 January 2022; Received in revised form 21 August 2022; Accepted 27 August 2022
Available online 31 August 2022

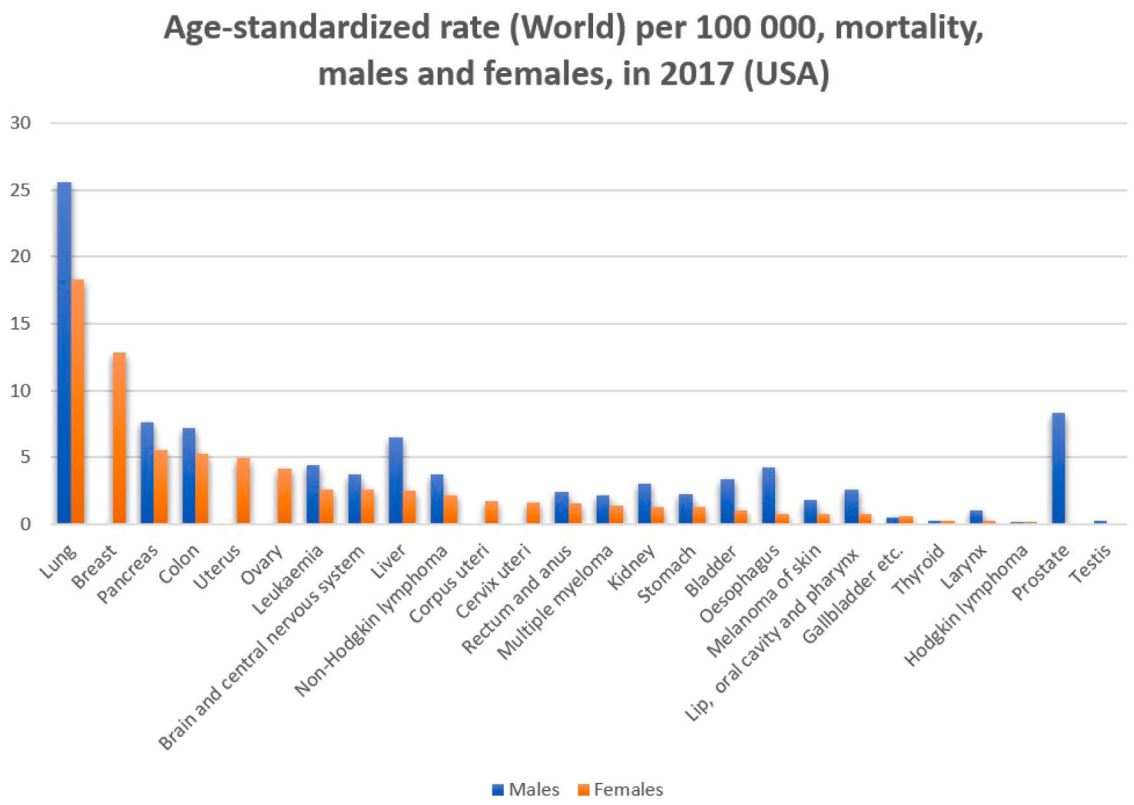


**Fig. 1.** Mortality rate due to various types of cancers.[1]

BC can invade nearby healthy tissues and make their way into the underarm lymph nodes, they then have a pathway into the other parts of body. BC stage refers to how far the cancer cells have spread beyond the original tumor. 85%–90% of cancers have their roots in genetic abnormalities brought on by the ageing process and general "wear and tear" living. The exact cause is unpredictable and is hard to answer why a woman has BC, whereas some do not have it. However, it is said in the studies that BC is caused when the DNA inside the cell is damaged/mutated. "Invasive Carcinoma", "Ductal Carcinoma", and "Invasive Lobular Carcinoma" are the three main categories of BC. The most prevalent type of BC is "Invasive Carcinoma", which originates in the milk ducts and propagates the surrounding tissues. "Invasive Lobular Carcinoma" is a type of Invasive Carcinoma that develops in glands.

### 1.1. Various imaging modalities for Breast Cancer detection

Accurate and precise diagnosis of BC is vital for the timely detection of cancer to improve survivability [1]. Many imaging modalities are continually being developed to diagnose this disease as early as possible. Medical images are the key source of information for the recognition and diagnosis of cancer diseases. Some of these modalities are used for screening purposes, some for diagnostic purposes, and a few others for adjunctive evaluation to provide field experts an additional confidence in their initial decision. The currently used imaging modalities for the diagnosis of BC are: "Mammography", "Ultrasound", "Histopathology", "MRI", "CT", "Positron Emission Tomography" (PET) and "Thermography" (see Fig. 3). Each of these imaging modalities has its significance.

#### 1.1.1. Mammography

Mammography is the most commonly used method to diagnose BC in women with no signs of diseases. Mammography is the golden standard to diagnose the Breast Cancer at an early stage. Mammograms are the x-ray images of the breast. It employs low-energy x-rays for breast examination and screening [2]. Being sensitive to calcifications, Mammography has achieved far better results in detecting micro-calcifications and clusters of calcifications [3]. Mammography is the ideal method for detecting "Ductal Carcinoma In Situ" (DCIS). "Carcinoma in situ" was diagnosed in 78.9% and 68.4% of patients using Mammography and MR Mammography, respectively [4]. In randomized controlled trials involving the general population, the Mammography screening test has been proven to reduce death rates [5]. Mammogram images have demonstrated to be technically more suitable for screening and, as a result, they can be employed for routine screening [6]. Furthermore, the fundamental Mammography technique has been amended to provide 3D scans of the breast in "Digital Tomosynthesis Mammography". "Contrast-Enhanced Digital Mammography" (CEDM) is a recent advancement in Mammography that uses an intravenous infusion of an iodinated contrast agent together with a Mammography examination [7].

#### 1.1.2. Ultrasound

Unlike other imaging modalities, Ultrasound images are generally monochrome and low resolution images. Ultrasound images of malignant regions are typically irregular in shape, blurred and vague margin. Ultrasound can successfully identify cysts from solid masses, whereas mammography cannot [8]. Furthermore, Ultrasound is more responsive in dense breasts and has proven to be an excellent mammography scanning tool [9]. The existence of speckle noise, however, is an intrinsic characteristic of ultrasound images [10], which degrades the performance of ultrasound images.

#### 1.1.3. MRI

Among breast imaging techniques, Magnetic Resonance Imaging (MRI) has the highest sensitivity. MRI efficiently displays the shape, size, location of breast lesions as they support multi-planner scanning and 3D reconstruction techniques [11]. However, MRI is time-consuming and of high cost. Supplementary to Mammography, MRI is

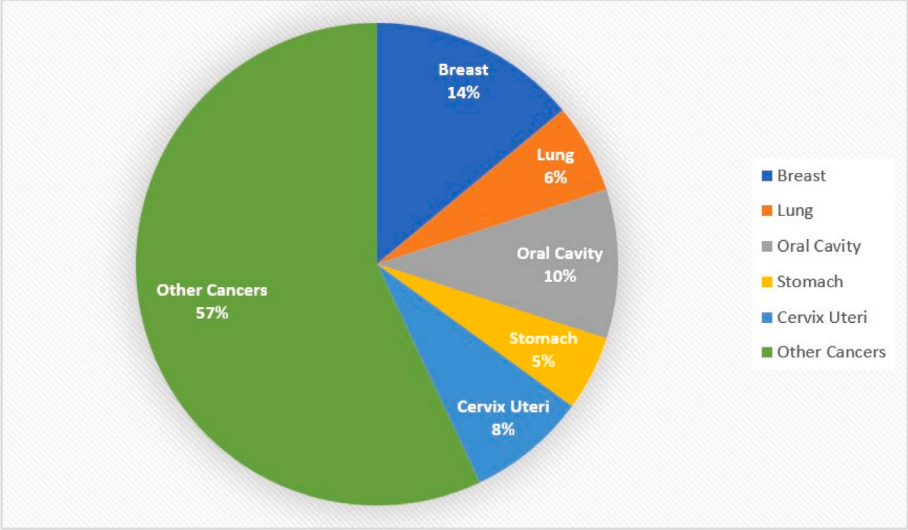


**Fig. 2.** Cancer statistics for year 2018.

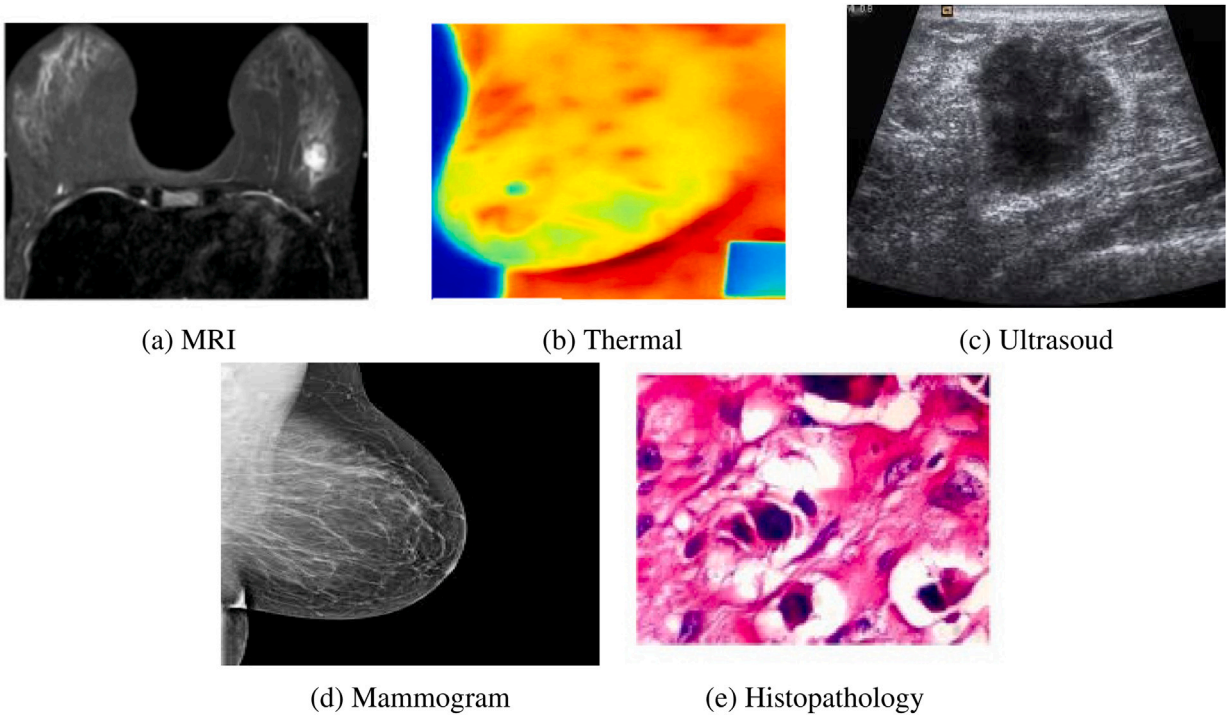


**Fig. 3.** Breast tissue medical images: (a) MRI (b) Thermal image (c) Ultrasound (d) Mammogram (e) Histopathology.

predominantly used for BC screening. For BC patients especially with pulmonary symptoms, CT images have been widely used for preoperative staging of patients. CT images had been useful in predicting lymph node metastasis.

### *1.1.4. Histopathology*

In comparison with [12] other medical imaging, Histopathology is considered the golden standard for BC diagnosis. They carry phenotypic information and are critical for the diagnostics and medicament of cancer disorders. However, for BC multi-classification, Histopathology Images (HI) have huge limitations: high coherency of cancerous cells, high intra-class difference, and low inter-class difference. Furthermore, same class images have greater resolution, contrast, and large appearance difference with respect to different class images [13], which leads to difficulties in distinguishing the types of BC. In addition, the gigapixel Whole Slide Images (WSIs) have high resolution, greater than 1 GB each, therefore the huge size of WSIs is a challenging task for DL models to process them in their entirety.

### *1.1.5. Thermography*

Breast Thermography or Thermal Imaging is an another imaging modality for BC diagnosis, where heat patterns are significant indications of breast abnormalities due to the increased quantity of heat created by malignant cells. Breast Thermography, unlike other Breast Cancer imaging modalities, is painless, non-invasive, non-contact, and harmless to both the thermographer and the patient, therefore it can be used for annual medical check-ups [14]. Thermography in conjunction with Mammography is used for early detection of BC. However, Mammography is recommended for young women due to low contrast images of dense breasts. At the early stages of cancer, researchers have

**Table 1**
Advantages and disadvantages of different BC imaging techniques.

| Imaging modality | Advantages | Disadvantages |
|---|---|---|
| Mammograms | Mammography is the standard imaging modality for early detection of BC. Mammograms are highly sensitive for fatty tissues. | Mammograms have lesser sensitivity for high-density breasts or younger women. Ionizing radiation escalate the risk of developing BC, limiting the use of Mammography as a routine screening tool. Mammograms are expensive and have less specificity. Furthermore, the breast region must be compressed in order to obtain precise mammograms, which can cause fear and pain in some people. |
| Histopathology Images(HI) | HI cover the detailed view of diseases and is considered the golden standard in diagnosing all types of cancers. | Analyzing HI is a challenging task due to their inconsistent staining, illumination variation and, overlapping. Moreover, the huge size of HI is a challenge for DL models to process them in their entirety. |
| MRI | Beneficial for the women possessing high risk factor. | Malfunctioning of medical devices for patients with metallic devices. They have low specificity and are costlier than ultrasound and Mammogram imaging |
| Ultrasound | Ultrasounds do not utilize radiations and are non-invasive. These are suitable for patients with dense breasts | Ultrasound images have poor resolution and do not cover the entire breasts. |
| Thermal | Breast Thermography is painless, non-invasive, non-contact, and harmless to both the thermographer and the patient and, can be used for the early detection of BC. Thermography is convenient for dense breasts. | Thermography do not detect BC, it only alerts a person about changes and patient need to go for further investigation. |
| PET/CT | PET/CT images are more effective in identifying distant metastasis due to their high sensitivity and specificity. | PET/CT images are less suitable for small breast lesion detection and early detection of BC. |

shown that thermography-based techniques can diagnose cancer 8–10 years earlier than Mammography [15]. Infrared Thermography is employed for different cancer detection processes at the preliminary stage including Breast Cancer, Brain tumor, skin cancer, etc. In addition to cancer detection, it can also be used for the diagnosis of various diseases that include Liver diseases, Diabetes diagnosis, Eye Ocular issues, and novel COVID-19 virus [16]. Table 1 demonstrates the advantages and disadvantages of various imaging modalities.

The examination of medical images for BC diagnosis by field experts such as pathologists, radiologists is a sensitive process and requires ample time and high qualification. There are certain limitations for qualitative analysis of medical images: absence of skilled pathologists, manual evaluation of millions of cells that could drop the mental focus leading to misdiagnosis, time-consuming and tedious tasks. The increased global demand for the early diagnosis of BC has opened up new research opportunities over the last 10 years [17]. Early detection of BC considerably increases the likelihood of making better treatment decisions. Medical imaging diagnosis can benefit from the use of Computer-Aided Diagnostic (CAD) systems. BC detection and localization are made easier with the use of CAD systems. CAD systems make use of computer algorithms to facilitate interpretation of images. Various Studies [18] demonstrated that CAD-assisted software produce low sensitivity (generate large number of false positives) and does not improve accuracy. Prior reports have also confirmed that not all cancers are marked by CAD and that cancers are overlooked more often if CAD fails to mark a visible lesion. To a great extent, Moore's law (processing power doubles every two years) [19] directly promotes progress of Computer-Aided Diagnosis systems. The performance of CAD systems has improved due to faster and cheaper hardware, which allows intensive computation for large datasets.

Artificial Intelligence (AI) assisted CAD systems have shown great potential applications in different fields of healthcare industry [20,21]. However, there have been very few reports of clinical benefits that have come up from the usage of AI in clinical practice, meaning that the potential of AI in healthcare has not yet been realized. This makes it difficult to evaluate the efficacy of AI in this field. The two main challenges that impede the adoption of AI based techniques in clinical practices are: (1) Inability of ML and DL models to generalize in complicated and real complex medical datasets. (2) Limited availability of labeled high quality datasets, emerging restrictions, and ethical and legal constraints over data sharing all play a role in the development of therapeutics [22]. The only studies that have shown AI to have any promise are retrospective ones. However, prospective studies and external validations are required in order to translate these potentially cutting-edge technologies from the research stage into the clinical practice setting.

### 1.2. Motivation and paper structure

The primary objective of this research study is to encourage field specialists (radiologists and pathologists) to use DL approaches for accurate BC diagnostics and evaluation. This article gives an overview of various DL algorithms practiced for BC detection, segmentation and classification using multiple imaging modalities including "Mammography", "Histopathology", "Ultrasound", "MRI", "PET/CT", and "Thermography". We review the publicly available datasets of different imaging modalities employed for BC detection to make future research more accessible. Furthermore, this is the first research study that explores the Deep Reinforcement Learning for Breast cancer diagnosis.

Following is the structure of this review paper: Section 1 introduces the Breast Cancer and various Breast Cancer imaging modalities, Section 2 briefly discuss the background of Deep Learning architectures. Sections 3–8 discuss the review work of the studies conducted for BC diagnosis using ML and DL techniques on Mammography, Histopathology, Ultrasound, MRI, PET/CT, and Thermal Imaging datasets, respectively. Section 9 briefly introduces the Deep Reinforcement Learning algorithms applied for BC detection. Section 10 highlight the DL challenges and future directions ahead for Medical Image Analysis (MIA), Section 11 provide the brief discussion of our research study, and finally Section 12 concludes this research review. Fig. 4 represents the roadmap(papers structure) of our research study conducted for breast cancer diagnosis.

### 1.3. Article selection criteria

We explored research studies published between 2015 and 2021 to: (1) assess the usage of various imaging modalities, (2) compare BC imaging modalities, and (3) identify the most cited and publicly accessible BC databases with different types of BC (4) Evaluate the applicability of Deep Learning in MIA, with a focus on BC, and (5) evaluate the applicability of Deep Learning methods on various BC imaging modalities. "Deep Learning", "Machine Learning", Breast Cancer Diagnosis", "Breast Cancer Imaging modality", "application of Deep Learning for Breast Cancer", "Deep Reinforcement Learning for Breast Cancer diagnosis", "Medical Image Analysis" were the keywords generally

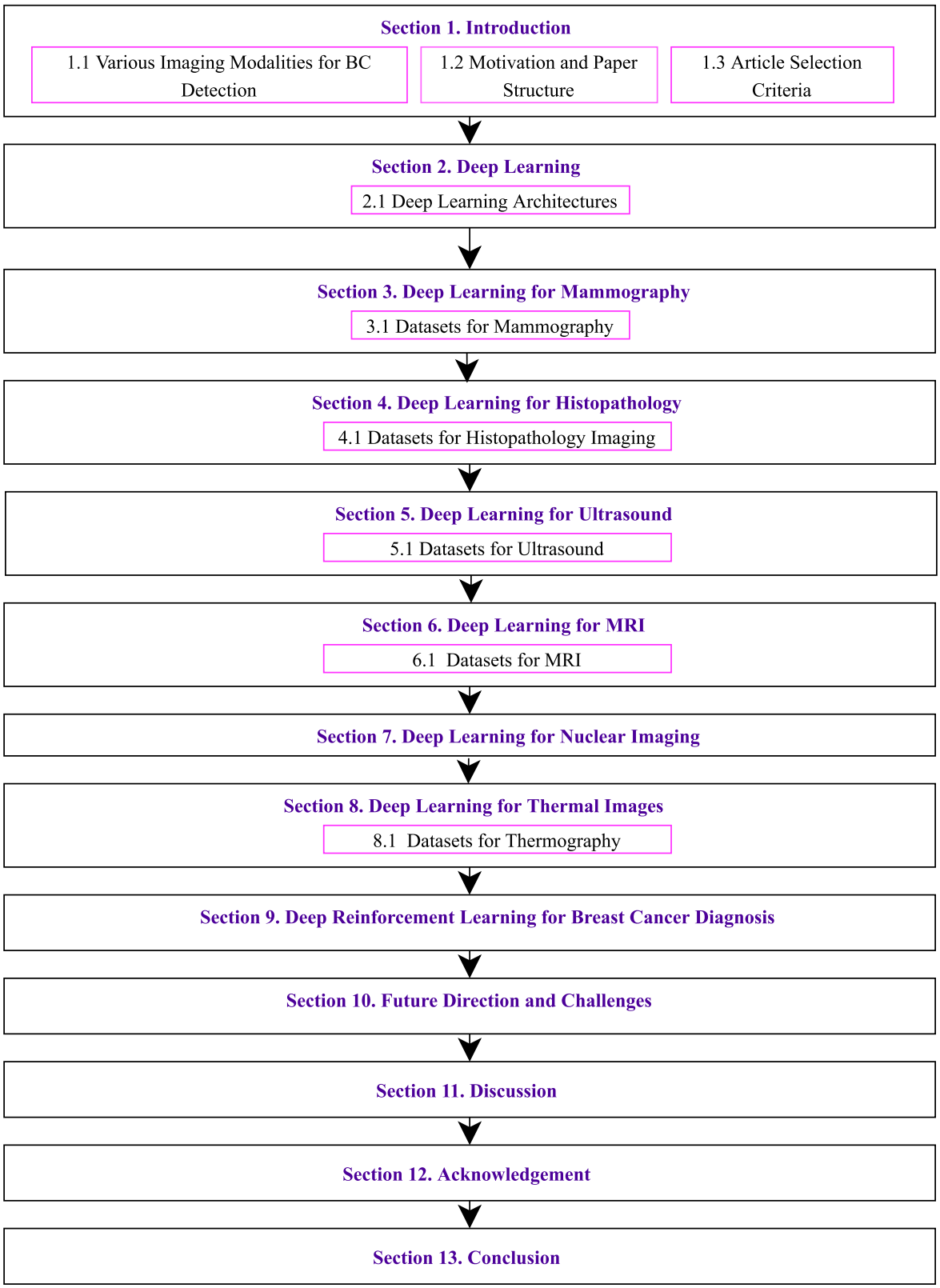


**Fig. 4.** Paper roadmap.

used as searching criteria in this research study. Studies were retrieved by searching seven databases including Science Direct, PubMed, Web of Science, ArXiv, SPIE, IEEE Xplore Digital Library, and Google Scholar. Furthermore, statistics for mortality rate due to various cancer diseases was collected from Global Cancer Observatory.[1] Fig. 5 demonstrate the paper searching strategy employed for conducting the research on Breast Cancer diagnosis.

The paper searching strategy for exploring the research conducted on Breast Cancer diagnosis using AI based techniques went through three phases: (1) Identification Phase (2) Evaluation Phase and (3)

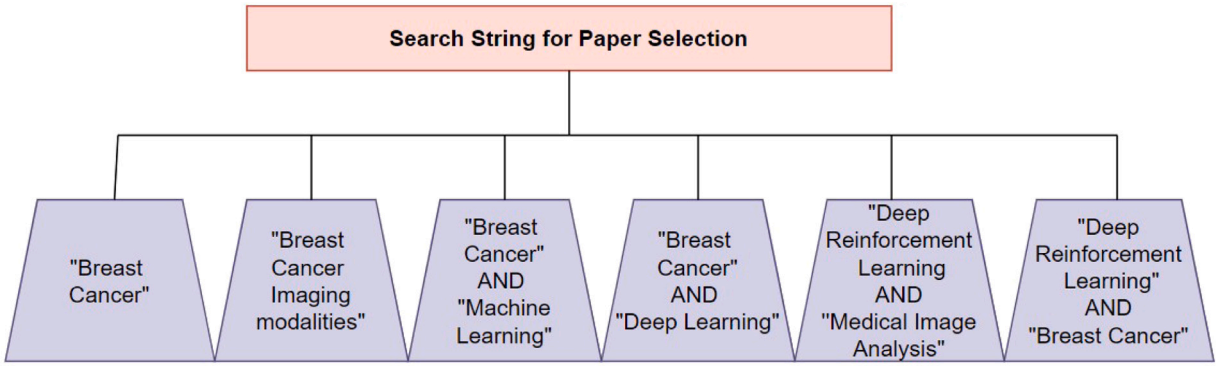


**Fig. 5.** Paper searching strategy.

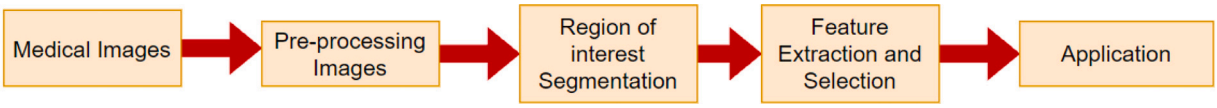


**Fig. 6.** Handcrafted feature extraction method.


**Fig. 7.** Deep learning feature extraction method.

Selection Phase. In the Identification Phase, 600 papers were selected. In Evaluation Phase, only 400 papers were selected, after removing remaining papers either because of their redundancy or irrelevancy. In Selection Phase, 200 papers were selected after reading the abstract, introduction and conclusion of research articles.

## 2. Deep learning

ML has recently gained its popularity in research, with applications ranging from text mining [23] to spam detection [24], video recommendation [25], and image classification [26]. Amongst the various ML algorithms, DL is the most commonly used technology in these applications [27–29]. DL unlike previous Machine Learning (ML) approaches, learn features on its own. Previously, handcrafted feature extraction techniques were used to extract and select features (such as "wavelet", "shape", "geometric", and "texture"). After manual segmentation, these approaches extract features from the regions-of-interest (ROI) (as shown in Fig. 6). Then, to obtain the final findings, traditional ML models such as "Support Vector Machines" (SVM), "Decision Trees" (DT), "Random Forest", "Naive Bayes", and "Adaboost" are used. However, this traditional hand-crafted feature extraction method is a tedious task and takes a long processing time. DL, in comparison to classical ML, is an end-to-end processing method that produces faster and more accurate results by extracting high-level characteristics directly from image data. From image data, DL models learn hierarchical characteristics. DL models are composed of numerous layers that acquire the features of an image in depth [30]. The initial layers of the DL model extract generic attributes (e.g., edges,blobs,circles), the intermediate levels extract mid-level features (eyes,nose,mouth) and the last layers extract high-level features (e.g., objects like head) [31] (as shown in Fig. 7). DL is most known for its ability to correctly classify and segment images. Medical researchers have been motivated by the widespread use of DL in the detection of natural images and have begun to investigate its application in the medical field. DL techniques have been applied to various medical specialties, particularly in the field of radiology and pathology [32]. In recent research studies [33–36], DL based framework Convolutional Neural Networks (CNNs) showed promising results in cancer detection and diagnosis. These models have been widely utilized to detect and classify cancer using images from Mammography, CT, Ultrasound, MRI, Histopathology, and Thermography.

### 2.1. Deep learning-based architectures

In DL terminology, "Supervised learning" is referred to as Discriminative technique, while as "Unsupervised learning" is called Generative technique. The discriminative DL model is applied directly to medical images, extracting the features from the image data. A generative model, on the other hand, creates new data by learning the characteristics of visual data. Various discriminative and generative models can be seen in Fig. 8. The main achievement in the field of Artificial Intelligence that allowed us to detect malignant tumors was the creation of "Artificial Neural networks" (ANNs). ANN is a network of neurons influenced by the working of the human brain, that receives the input, processes it, and accordingly produces the output as shown in Fig. 9(a). ANN constitutes three parts: "input layer", "dense layers", and "output layer" (see Fig. 9(b)). The information is fed into the input layer, which is then processed by the neural network. Dense layers process the data and can be of any number. Each dense layer is made up of neurons. These neurons receive information from the previous layers, multiply it by weight, and then add a bias to these. The output layer combines all the information from the last hidden layer to produce the desired output. The predicted output is compared to the target output to calculate the error. The entire goal of training is to minimize the error and this is done using a process called "Backpropagation". The "Backpropagation" mechanism uses the "Gradient Descent Algorithm" to update the weights of the neural network architecture in order to minimize the error between predicted and actual output.

The most standard model of DL is the "Convolution Neural Networks" (CNNs). With enough training data, CNNs can learn extremely representative and layered hierarchical characteristics of an image. It is a highly preferred neural network for image classification and

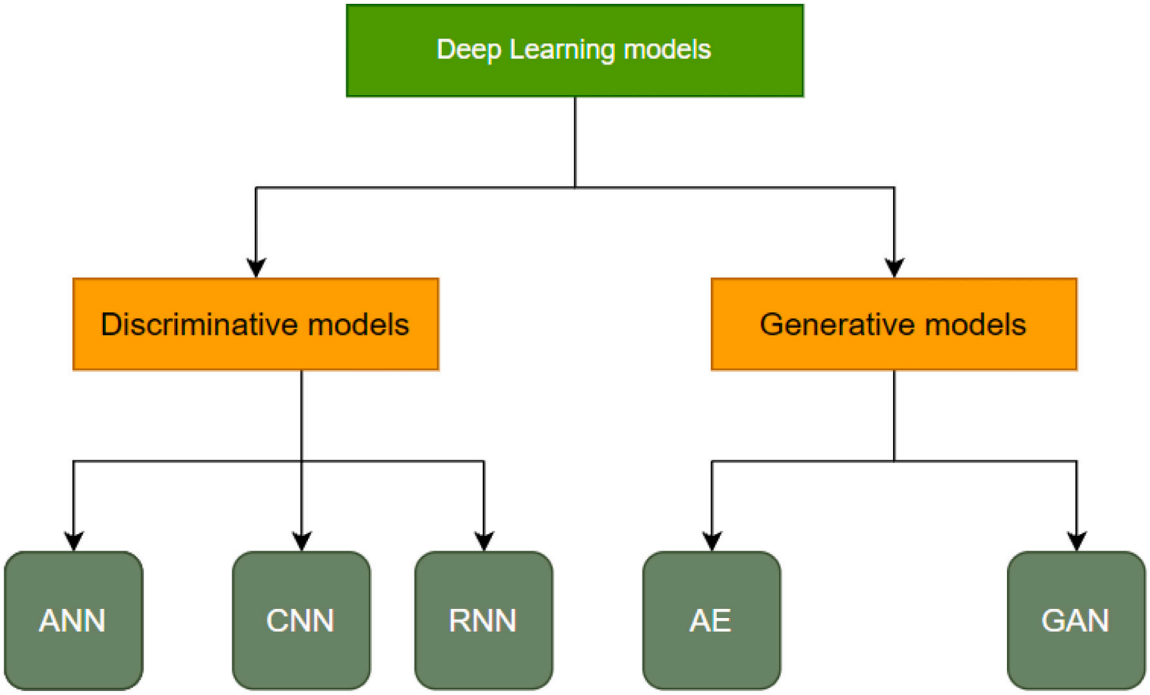


**Fig. 8.** Deep learning architectures.

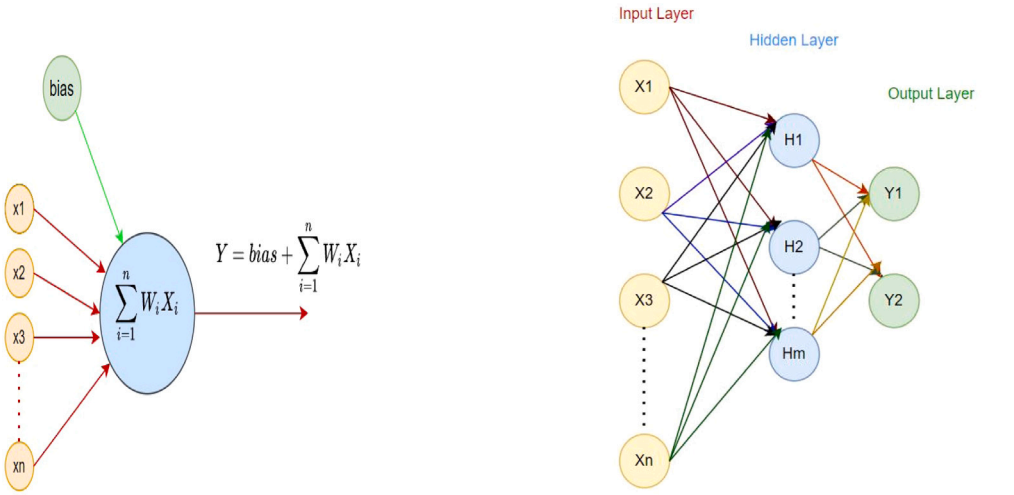


**Fig. 9.** Represents the artificial neuron and artificial neural network architectures.

has attained great performance for Medical Image Analysis (MIA) and classification [37]. Apart from MIA, CNNs are widely used in a variety of fields including computer vision [38], face recognition [39], natural language processing (NLP) [40], audio and video processing [41]. Parameter sharing and sparse connections are the key benefits of CNN architecture [42]. It makes use of filters to extract efficient features from image pixels. The basic CNN model consists of multiple Convolution layers (filters/kernels), Pool layers (down-sampling), Fully connected layers (Dense layers), and activation functions (e.g., ReLU, Sigmoid, Tanh, Softmax) as shown in Fig. 10 [43]. The convolutional layer makes use of filters. In each region where the filter passes, a single value is obtained by performing the mathematical (Convolutional) operations on the input image. To overcome the "Vanishing Gradient Problem", the activation function typically the ReLU activation function is applied after each convolution layer. The pooling layer is grounded on the "Sliding Window" principle. The main functionality of the pooling layer is the dimensionality reduction. Generally, there are three pooling methods "Max Pooling", "Average Pooling", and "Sum Pooling". The preferred choice is the Max Pooling. In Fully Connected (FC) layers, all nodes in the layer are connected to each node in the previous layer. The main purpose of the dense layers is to perform the classification of the features that are extracted from the convolutional and pooling layers. In the last dense layer, each target class contains a single artificial neuron and a probability value between 0–1 is generated with the "Softmax" activation function for each neuron. Model architecture has great impact in improving the performance of various applications. "AlexNet" [44], "Visual Geometry Group Network" (VGGNet) [45], "ResNet" [46], "GoogLeNet" [47] are some classical supervised learning CNN models that have won top computer vision challenges. Fig. 11 shows top 5 error rate of various

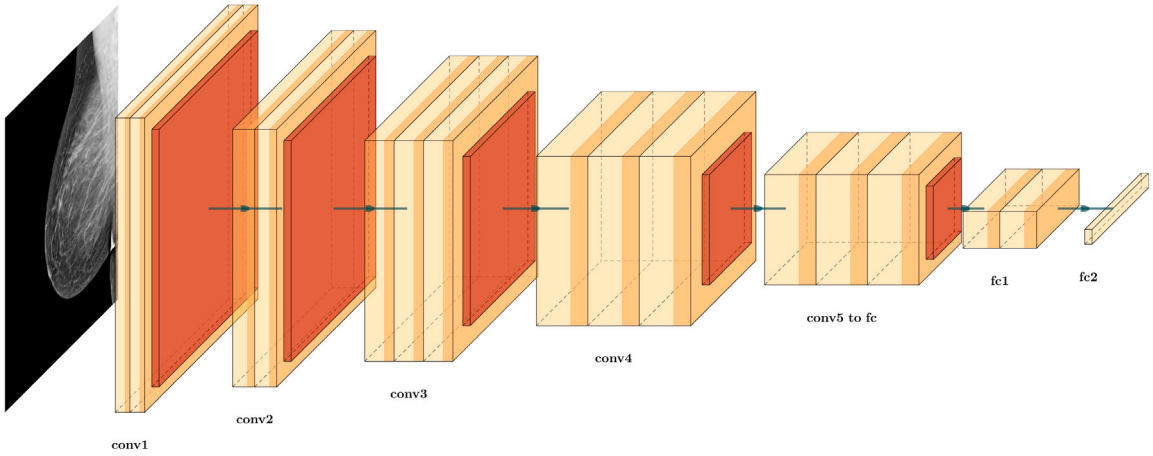


**Fig. 10.** Structure of CNN for medical image classification.

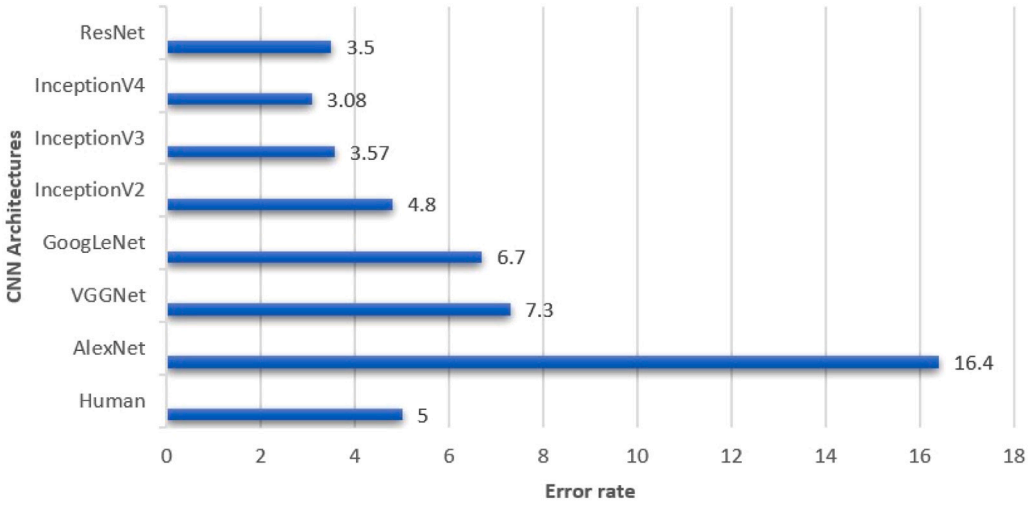


**Fig. 11.** Comparision of CNN architectures with human level performance.

CNN architectures on ImageNet [48] dataset. All these models were evaluated on a large dataset (ImageNet). CNN models exceeded the human performance in various computer vision tasks such as image recognition.

The evolution of CNNs started with the introduction of LeNet [43] architecture, initially the CNNs were confined to handwritten numeral classification task, which could not be generalized to all image classification tasks. "AlexNet" proposed by [44] achieved remarkable results in image recognition and classification tasks by increasing the depth of model and employing different parameter optimization techniques. At that time, the learning capability of CNNs was restricted by hardware limitations. Therefore, "AlexNet" was trained on two GPU's in parallel. Increasing the depth of network gave rise to overfitting problem. To address this problem, the authors employed Local Response Normalization (LSN) and overlapping subsampling techniques to ensure robust features are learned by the model. "VGGNet" [45] is a multilayered architecture with 19 more layers than AlexNet architecture. "VGGNet" utilizes small filters of size $3 \times 3$, which produces the same influence as large size filters ($5 \times 5$ or $7 \times 7$) and decreases the number of parameters thereby decreasing the computational complexity. However, the major drawback of VGGNet is huge parameter utilization around 140M that makes it computationally expensive. The main aim of "Inception-V1(or GoogleNet)" [49] was to design a highly generalized model with low computational cost. A new concept (Inception block), which employs merge, transform, and split functions for feature extraction was first time introduced in the CNN world. Furthermore, to speed up the convergence rate, Inception-V1 presented the concept of auxiliary learners. However, GoogleNet also suffers from two short comings. One is the heterogeneous topology and the another one is the representation jam. "ResNet" [46] architectures have been widely used for image classification. One problem that ResNets solve is the "vanishing or exploding gradient problem". ResNet model has numerous architectures in the context of the number of layers and parameters for the ImageNet dataset, which are ResNet18, ResNet34, ResNet50, ResNet101, and ResNet152 [46]. "Inception: ResNet, Inception-V3, and Inception-V4" [50,51] are the modified versions of Inception-V1 and Inception-V2. The authors here employed asymmetric filter size ($1 \times 5$ or $1 \times 7$) rather than large size filters($5 \times 5$ or $7 \times 7$). On the other hand, in Inception-ResNet the filter concatenations were replaced with the residual connections. Various CNN architectures with their configuration are shown in Table 2.

Training of CNN models requires a large dataset for improving the performance. However, amount of annotated medical image datasets is very less and small datasets are not sufficient to train these CNN models and may potentially result in an over-fitting problem. Moreover, training these models from scratch takes many efforts in fine-tuning CNN parameters and takes a long time for training the model in comparison to the pre-trained models. Therefore, pre-trained models are used in place of training the models from scratch using transfer learning. Another supervised deep learning model is the "Recurrent Neural Network" (RNN) [53]. RNN remembers its input due to the internal memory, making it suitable for solving sequential data problems

**Table 2**
Different CNN models.

| CNN models | Number of layers |
|---|---|
| LeNet-5 [43] | 7 layers: 2 Convolutional layers (Conv2D), 2 pooling, and 3 Fully Connected (FC) layers. |
| AlexNet [44] | 8 layers: 5 Cov2D layers and 3 FC layers. |
| VGGNet-16 [45] | 13 Conv2D and 3 FC |
| Inception-V1 [49] | 22 layers with 5M parameters. |
| Inception-v3 [50] | 48-layers with less than 25M parameters and is the predecessor of Inception-V1. |
| ResNet-50 [46] | 5 layers with 23.51M parameters. |
| Inception-ResNets [51] | 164 deep layers. |
| Xception [52] | 36 Conv2D. |

(see Fig. 12). Therefore, RNN can be used for processing 3D volumetric images e.g., MRI images.

Unsupervised learning models including "Auto-Encoder" (AE), "Generative Adversarial Networks" (GANs), and "Deep Belief Networks" (DBNs) extract knowledge from unlabeled datasets. AE is an encoder–decoder-style neural network where an encoder transforms each image into the latent space and the decoder regenerate the image using learned features to acquire the information of raw features [54]. There are various models of auto-encoder including simple AE, Sparse AE, Deep Fully Connected AE, Deep Convolutional AE, Image Denoising AE, Sequence-To-Sequence AE, and Variational AE. Rooted from game theory, Generative Adversarial Network (GAN) is one of the most interesting topics in computer science. GAN is composed of two neural networks that are trained simultaneously. A generator that learns to generate artificial images and a Discriminator that discriminates real images apart from fake images [55]. GANs are very powerful as they can learn any kind of data distribution. The main drawbacks of unsupervised learning models are computationally expensive and unable to provide precise information regarding data sorting. In 2013 and 2017, MIT Technology Review nominated DL and Reinforcement Learning (RL) as one of the top 10 breakthrough technologies. RL is a method of learning a sequence of actions that maximize the expected reward [56]. Fig. 13 represents the framework of Deep Reinforcement Learning (DRL). DRL is a type of RL that amalgamates the DL and RL [57]. Thanks to DRL, RL may now be scaled up to previously unimaginable tasks. The amalgamation of these two powerful technologies is now one of the most cutting-edge artificial intelligence frameworks. In recent years, DRL has witnessed significant performance improvement in many areas, including computer vision [58], robotics [59], games [57], and Natural Language Processing (NLP) [60]. In Medical Image Analysis (MIA), DRL has been used to solve the problems like landmark detection [61], image registration [62], and view plane localization [63]. Besides parametric MIA problems, DRL has also been used for lesion detection/classification [64] and lesion segmentation [65,66]. The main advantage of DRL is for small and imbalanced datasets. For imbalanced datasets, DRL can provide effective solution for classification task.

Despite its tremendous success, DRL has not been fully explored in Medical Image Analysis (MIA). The major disadvantage of DRL is the hyperparameter tuning that can affect the speed of learning. Another disadvantage that constraint the usage of DRL for image analysis is that, DRL is computationally expensive and time consuming for large datasets.

In this research study, Deep Learning supervised models (CNN, RNN), unsupervised models (AE,GAN) and Deep Reinforcement Learning models were reviewed for the diagnosis of BC using different Imaging modalities. Pre-trained models like ResNet, AlexNet, InceptionV3, InceptionResNetV2, DesNet, VGG16,GoogLeNet were also reviewed for the diagnosis of BC. U-Net architecture is studied for the segmentation of BC to improve detection and classification performance. From ML perspective, classification algorithms like DT, KNN, NB and SVM are also studied for BC classification.

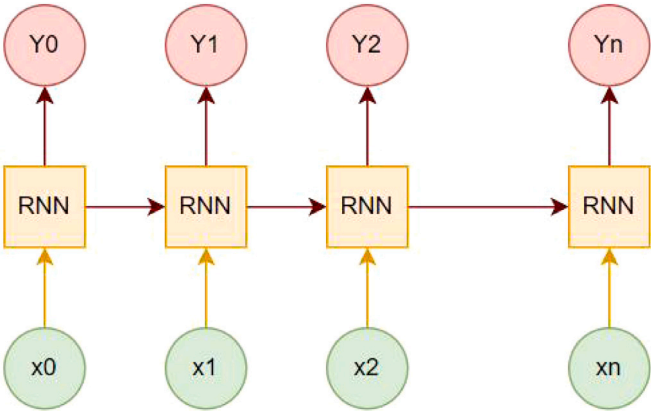


**Fig. 12.** Recurrent neural network.

## 3. Deep learning for Mammography

The section presents the recent literature on ML and DL for four discernible Mammography tasks:breast density classification, calcification detection and classification, breast asymmetry detection and classification, mass detection and classification. A tremendous number of Mammogram datasets are available, that can be used to analyze the hidden new patterns for the early detection of diseases [67]. Support vector Machine(SVM) is a supervised ML algorithm and has been widely employed for image classification. In [68–73] research studies, the authors employed SVM for breast mass detection and classification. All these research studies were conducted on DDSM dataset. A simple CNN has been applied by [74] to learn the features for the classification of a breast mass. In comparison with the hand-crafted feature extraction methods, this model showed an increment in terms of AUC from 79.9% to 84%. [75] applied two well-known CNN models for benign and malignant classification of Mammogram images. The accuracy results of VGG-16 (94%) were higher than ResNet50 (91.7%). A modified AlexNet architecture has been presented by [76] for categorization of Mammogram images into benign and malignant using the Mammographic Image Analysis Society (MIAS) dataset. The proposed model gives an overall accuracy of 95.70% showing an improvement over the traditional method (without augmentation) with an accuracy of 80.32%.

Among multiple features extracted from Mammogram images, the density feature is highly related to BC. [77] employed a light-weighted CNN model to classify Mammogram images based on BI-RADS density using the MIAS dataset and achieved an average accuracy of 83.6%. To enhance the effectiveness of conventional CNNs, [78] employed dilated and attention-guided residual learning on INBreast imaging dataset. The dilated CNN improves the receptive field of a network while ensuring image quality. This method uses multimodal detection to extract characteristics from bilateral MLO and CC images before feeding them into the CNN model for breast density classification. This multimodal technique exemplifies a developing trend in CNNs to improve model performance by combining several input sources. [79] proposed a hybridization approach of CNN and Radial Bias Function (RBF)-based SVM classifier in which the Transfer-Learning concept was used. In their work a CNN model was pre-trained on MRI spine images and then the spine CNN was fine-tuned and retrained on a few malignant and benign breast images. Finally, an RBF-based SVM classifier has been applied for the classification of breast images. From the comparison, the accuracy result of this hybridization model (92%) was higher than AlexNet (85%) and GoogLeNet (77%). Therefore, we can conclude that combining DL models with classic ML approaches provides Promising DL architectures. [80] described a DL-based Multi-view Neural Network (MV-NN) architecture for the classification of

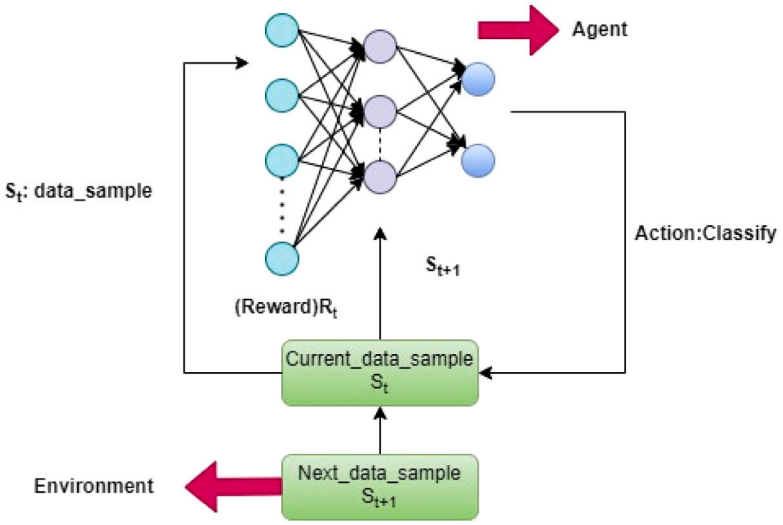


**Fig. 13.** Deep reinforcement learning framework.

microcalcifications as benign and malignant. This work was carried out on a large number of samples extracted from Digital Database for Screening Mammography (DDSM dataset) that consists of multi-view images. The MV-NN approach outperformed all other methods such as Logistic Regression (LR), Support Vector Machines (SVM), EM-LR simple Neural Network (NN), and EM-NN. A regional DL-based technique You Only Look Once (YOLO) has been proposed by [81] for the detection and classification of a breast masses. YOLO combines the information of many Mammograms into a single neural network to simultaneously detect and classify Breast Cancer.

A novel Autoencoder (AE) model was firstly suggested by [82] for the classification of BC with Mammography. Each layer of this model uses the sigmoid function, except the last layer, which uses the Linear Transformation function. Two optimization methods including Mean Classification Error (MCE) [83] and Mean Squared Reconstruction Error (MSRE) [84] has been employed for the extraction of features. [85] presented an architecture called "Convolutional Sparse Autoencoder" (CSAE) for Mammographic density scoring. The proposed model consisted of Sparse Encoder [86] within a CNN, using deep features in an unsupervised way. To control model capacity "Sparsity Regularization" has been employed. GAN can be used for augmentation purposes. [87] presented Autoencoder-Generative Adversarial Network (AGAN) for enhancing the data delivered to the CNN classifier by generating an additional representation of Mammogram images. The proposed system has been used to distinguish normal images from abnormal with an accuracy of 89.71%. Table 3 demonstrates some studies conducted for BC on Mammogram images using DL techniques.

### 3.1. Datasets for Mammography

Most of the BC Mammographic datasets are not publicly accessible. The most easily accessible and commonly used Mammographic databases are: "Mammographic Image Analysis Society" (MIAS) Dataset, "Digital Database for Screening Mammography" (DDSM). Besides these databases, there are also some projects like IRMA which are designing and maintaining the Mammogram datasets.

#### 3.1.1. Image retrieval in medical applications

The Image Retrieval in Medical Applications (IRMA) [88] project intends to design and implement high-level algorithms for "Content-Based Image Retrieval" (CBIR), with a proposed application to medico-diagnostic activities. IRMA is a database of Mammogram images from "RWTH Aachens", in Germany. The Mammogram images are 128 × 128 pixels in size including 931 images as benign and 584 images as malignant. This Mammography database is composed of four different datasets, which are "Mammographic Image Analysis Society" (MIAS) a Digital Mammogram Database, "Lawrence Livermore National Laboratory" (LLNL), "Digital Database for Screening Mammography" (DDSM), and routine images from the "Rheinisch Westfalische Technische Hochschule" (RWTH) Aachen.

#### 3.1.2. Mammographic Image Analysis Society

The Mammographic Image Analysis Society (MIAS) Dataset [89] was designed by a UK based research group. The MIAS dataset consists of a total of 322 digitized images, with 207 images being normal and 115 images being aberrant. The original size of the image is 1024 × 1024 pixels. The dataset is splitted into two sections: training set and testing set, with 31% (100 samples) of the 322 samples practiced for training and 69% (222 samples) were employed for testing without applying any data augmentation. This database also includes the ground truth marking of the abnormalities present in the images.

#### 3.1.3. Digital Database for Screening Mammography

The Digital Database for Screening Mammography (DDSM) [90] is the largest available Mammogram database used for Mammographic image analysis. This database is the synergetic effort of "Massachusetts General Hospital", "Sandia National Laboratories" and the "University of South Florida Computer Science and Engineering". The Mammograms were acquired from "Massachussets General Hospital" (MGH), "Wake Forest University School of Medicine" (WFU), "Sacred Heart" (SH) Hospital, and "Washington University" (WU) of St. Louis School of Medicine. DDSM dataset contains 2620 examples, with two images of each breast.

#### 3.1.4. Breast Cancer Digital Repository

The IMED project, which was led by "INEGI, FMUP-CHSJ" at the University of Porto in Portugal and "CETA-CIEMAT" in Spain, helped to develop The Breast Cancer Digital Repository (BCDR) dataset [91]. The BCDR database comprises of 1734 BIRADS-classified cases. The BCDR is split into two phases (1) A "Film Mammography" based repository BCDR-FM, and (2) a full-field Digital Mammography based repository BCDR-DM. BCDR-DM consists of MLO and CC grey-scale digitized Mammogram images with a resolution of 720 × 1168 pixels saved in TIFF format. BDCR-FM contains 1010 cases of anonymous patients with 1125 studies, 3703 "Mediolateral" (MLO), and "Craniocaudal" (CC) Mammography incidences. BCDR-DM also contains MLO and CC grey-scale images with a resolution of 3328 × 4048 or 2560 × 3328 pixels saved in TIFF format.

**Table 3**
Studies conducted for BC based on Mammography using DL. AUC: Area under the Curve; Accu: Accuracy; Sens: Sensitivity; Spec: Specificity.

| Related work | Dataset | Input size | Model | Output performance |
|---|---|---|---|---|
| [74] | Dataset:BCDR<br>Benign:426<br>Malignant:310 | 150 × 150 | CNN | Accu:86% |
| [75] | Dataset:IRMA<br>Benign:931<br>Malignant:584 | 224 × 224 | VGG16+ResNet50 | Accu:94%, 91.7% |
| [76] | Dataset:MIAS<br>Total:2576<br>Training set:31%<br>Testing set:69% | 64 × 64 | AlexNet+Augmentation | Accu:95.70% |
| [77] | Dataset:MIAS<br>Total:322<br>Training set:80%<br>Testing set:20% | 200 × 200 | Light Weight CNN | Accu:83.6% |
| [79] | Dataset:private<br>Total:5147 | 227 × 227 | CNN+SVM | Accu:92.0, spec:0.86% |
| [81] | Dataset:DDSM<br>Benign:300<br>Malignant:300 | 448 × 448 | YOLO | Detection Accu:99.7%,<br>Classification Accu:97% |
| [80] | Dataset:DDSM<br>Total:705<br>Benign:372<br>Malignant:333 | -NA- | MV-NN+EM-NN | AUC:0.89,0.87,<br>Accu:78.7%,78.3 |
| [82] | Dataset:private<br>Total:949 | 128 × 128 | AE | Accu:98.45% |
| [85] | Dataset:private<br>Total:1576 | 24 × 24 | Sparse AE | AUC:0.61% |
| [87] | Dataset:DDSM<br>Total:11,218<br>Benign:444<br>Malignant:6774 | 32 × 32 | AGAN | AUC:0.9410,<br>Accu:89.71%,<br>Sens:93.54%,<br>Spec:80.58% |

#### 3.1.5. INBreast

The INBreast [92] Database consists of over 410 Mammograms images, collected from more than 115 patients. The database provides insights on types of abnormalities and mass contour information. Universidade do Porto no longer supports this dataset, but it is still available upon request.

#### 3.1.6. BancoWeb LAPIMO

The BancoWeb LAPIMO [93] dataset contains almost 1400 Mammogram images saved in TIFF formate. The images in this dataset are categorized as healthy, benign, and malignant.

## 4. Deep learning for Histopathology imaging

Histopathology is the golden measure of all imaging modalities. DL models in Histopathology accomplished better performance in segmentation, classification, and localization tasks. Some publicly available datasets as shown in Table 4 are being frequently used for the detection of BC by employing HI with DL models. In this section, we study various DL techniques that have been practiced on the available Histopathological datasets. Then, we epitomize the methods and results of our review work in 5.

DL based classification methods produce more convenient, precise and faster results when dealing with large amounts of data, as discussed in [94–97]. [98] proposed two magnification independent CNN models for the classification of Histopathological BC images. The proposed model includes: a single-task CNN model used for the prognosis of malignancy level and a multi-task CNN model used for magnification and malignancy level prediction simultaneously. The average recognition rate of the single-task CNN model for benign and malignant classification is 83.25%, Whereas the average-recognition rate of the multi-task CNN model in benign and malignant classification is generally 82.13% and 80.10% for magnification level prediction. The comparative analysis of various ML algorithms including "Support Vector Machine" (SVM), "Naive Bayes" (NB), "Decision Tree" (C4.5), and "K-Nearest Neighbor" (K-NN) was carried out by [99] on "Wisconsin BC" dataset using Weka software. SVM outperformed all the models with an accuracy of 97.13%. Transfer Learning (TL) also proved promising for BC diagnosis. [100] applied the TL concept using AlexNet CNN architecture on the "BreakHis" dataset for malignant and benign classification using HI. To solve the limited data availability problem, [101] employed augmentation and TL techniques with Google's "Inception V3" for BC classification. This model achieved an accuracy of 89%. [102] Proposed a DL framework for the detection and classification of cytology breast images using the TL technique. CNN-based pre-trained models including "GoogLeNet", "VGGNet", and "Residual Networks" (ResNet) have been to extract the features, which were then fed to the Fully Connected (FC) layer for the classification task using average pooling mechanism. The proposed framework outperformed all conventional models with an accuracy of 97.25%. [103] presented a multi-network classification framework to extract the significant visual characteristics for the classification of HI. Pre-trained multi-network Deep CNN (DCNN) models including "DenseNet-121", "ResNet-50", "multi-level Inception V3", and "multilevel VGG-16" have been used for feature extraction. The extracted features were high dimensional which can lead to high computational cost. Therefore, the "Dual Network Orthogonal Low-Rank Learning" (DOLL) model has been used for dimensional reduction. The authors applied fused features and voting strategy for classification purpose using Ensemble Support Vector Machine (E-SVM) classifier. [13] Proposed a non-linear Class Structure-based Deep CNN (CSDNN) model for the multi-classification of BC Histopathology Images. Some feature space constraints were designed and integrated with CSDCNN to control the feature similarities of different class images. This model achieved a patient-level accuracy of 93.2%, while as the image-level accuracy was 93.8%.

Scarcity of images demand the extraction of patches from high resolution Histopathology Images to increase the training dataset. [106] designed a patch based CNN classifier (PBC-CNN) for the classification of Breast Cancer HI. Mitosis detection is an essential characteristic for determining the severity of BC. [105] developed Deep Learning CNN-based framework for the mitosis detection on MITOS Histopathological Imaging dataset. A Cluster-based segmentation technique viz

**Table 4**
Datasets for Breast Cancer Histopathological imaging modality.
*Source:* Adapted from [104].

| Dataset | Year | Staining | Data size | Magnification |
|---|---|---|---|---|
| BreaKHis | 2015 | H&E | 7909 HI | 40×, 100×, 200×, 400× |
| Camelyon 2016 | 2016 | H&E | 400 lymph node WSIs | 40×, 10×, 1× |
| Camelyon 2017 | 2017 | H&E | 200 lymph node WSIs | 40× |
| TUPAC 2016 | 2016 | H&E | 500 training set and 321 testing set BC-HI WSIs | 40× |
| BACH | 2018 | H&E | 400 microscopy images and 30 WSIs | 40× |
| ICPR 2012 | 2012 | H&E | 50 images corresponding to 5 different biopsy slides | 40× |
| IDC | 2014 | H&E | 277,524 patches are from 162 IDC breast cancer histopathological slides (198,738 IDC negative, 78,786 IDC positive). | 40× |
| Bio-imaging Grand Challenge Dataset | 2015 | H&E | Training set of 249 images, test set of 20 images and an extended test set of 16 images | 200× |

**Table 5**
Studies conducted for BC based on HI using DL techniques. AUC: Area under the Curve; Accu: Accuracy; Sens: Sensitivity; Spec: Specificity, NA: Not Available.

| Related work | Dataset | Input size | Model | Output performance |
|---|---|---|---|---|
| [99] | Dataset:Wisconsin<br>Total:699<br>Benign:458<br>Malignant:241 | -NA- | SVM + DT + NB + KNN | Accu:97.13% |
| [105] | Dataset:MITOS<br>Total:1450<br>Mitotic:725<br>Non-Mitotic:725 | -NA- | CNN + SVM | Accu:96.8% |
| [13] | Dataset:BreakHis<br>Total:7909<br>Benign:2480<br>Malignant:5429 | 256 × 256 | CSDCNN | Accu :93.8% |
| [102] | Dataset:private<br>Dataset1: 7909<br>Dataset2: 8000 | -NA- | GoogLeNet + VGGNet + ResNet + Average pooling classification | Accu:97.52% |
| [103] | Dataset: ICIAR-2018 | 400 × 400 | DenseNet-121 + ResNet-50 + Inception V3 + VGG-16 | Accu:97.7% |
| [101] | Dataset: BreaKHis<br>Total: 11,184<br>Benign: 3504<br>Malignant: 7680 | -NA- | Inception V3 | AUC:0.93 |
| [106] | DataseT:ICIAR 2018 | 512 × 512 | PBC-CNN(OPOD+APOD) | Accu(OPOD):77.4%<br>Accu(OPOD):84.7%<br>Accu(APOD):90.0%<br>Accu(APOD ):92.5% |
| [107] | Dataset: DRYAD<br>Total:949 | 128 × 128 | U-NET | -NA- |

K-means has been utilized to extract the foreground cellular structure from HI. CNN model has been used for feature selection, and PCA (Principal Component Analysis) and Linear Discriminant Analysis (LDA) for feature reduction. Finally, the SVM classifier has been employed for mitotic and non-mitotic classification. The accuracy result for this methodology was 96.8%. Two pre-trained DCNN models including Inception-V3 and Inception-Resnet-V2 were adopted by [108] for BC detection using BreakHis dataset HI. Various data augmentation techniques were applied to address the imbalanced distribution of images in subclasses of BC. Furthermore, the authors designed novel unsupervised Auto-encoder (AE) model to reduce the dimensionality of features extracted by Inception-Resnet-V2 model, and to perform clustering analysis using the K-means algorithm on Histopathology Images. Region of Interest (ROI) segmentation is a challenging task on invasive cancer Whole Slide Images (WSIs), as invasive cancer cells are of low contrast and their appearance is very much similar to non-invasive regions [107]. Proposed the skipped connection-based U-Net Auto-encoder along with the concept of TL for the segmentation of Invasive breast cancer WSIs. An ensemble learning method was proposed by [109] to improve BC classification. The authors used gene-expression data and HI for classification task. Gene expression is the 1D data and was therefore converted into image data using Convex Hull algorithm [110] and t-Distributed Stochastic Neighbor embedding technique [111].

### 4.1. Datasets for Histopathology Imaging (HI)

#### 4.1.1. BreaKHis dataset

"BreaKHis" dataset [112] is the largest HI dataset containing 7909 breast biopsy samples from 82 anonymous patients of "Pathological Anatomy and Cytopathology" Lab in Brazil. This dataset is made up of benign and malignant tumor images, where the tumor images were taken on different zooming rates: 40×, 100×, 200×, 400×. This dataset consists of 1995 images of 40× magnification including 625 benign and 1370 malignant images, 2801 images of 100× magnification including 644 benign and 1437 malignant images, 2013 images of 200× magnification containing 623 benign and 1390 malignant and 1820 images of 400× magnification containing 588 benign and 1232 malignant images. "BreaKHis" dataset consists of eight subclasses of BC images categorized on the basis of diameter and shape of a cell. "BreakHis" dataset has four subcategories of malignant cancer: "Ductal carcinoma" (DC), "Lobular carcinoma" (LC), "Mucinous carcinoma" (MC), and "Papillary carcinoma" (PC), and four subcategories of benign cancer: "Adenosis" (A), "Fibroadenoma" (F), "Phyllodes tumor" (PT)

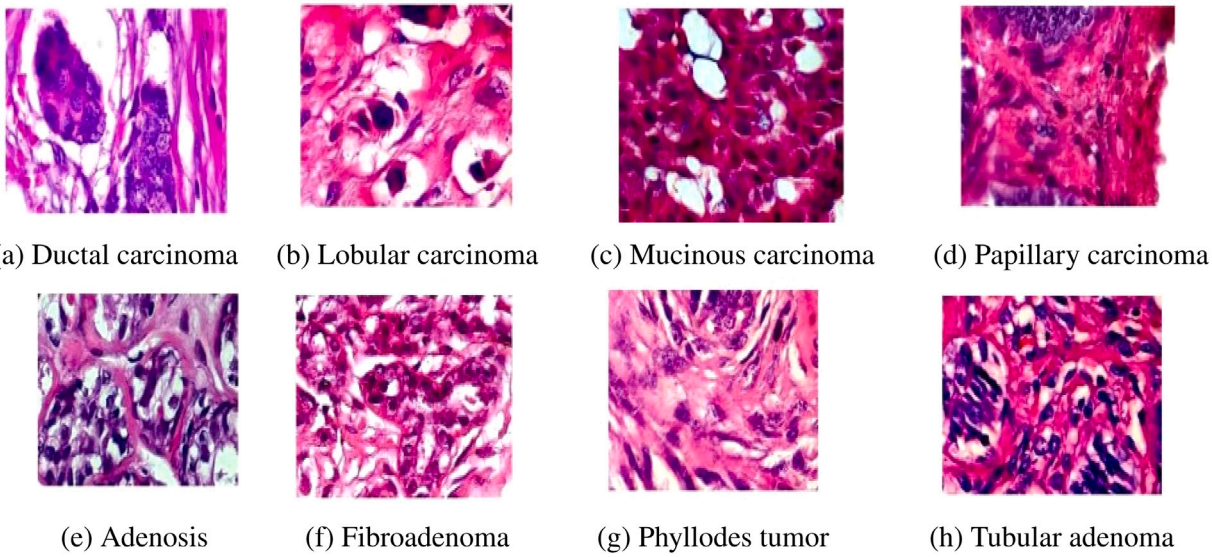


**Fig. 14.** Eight classes of Breast Cancer Histopathology images from BreakHis dataset [112].

and "Tubular adenoma" (TA) (see Fig. 14). The image pixel resolution is 700 × 460 and the image format is PNG. "BreaKHis" is the most commonly used database by researchers to carry out BC diagnosis using HI.

#### 4.1.2. Camelyon 16 dataset

Camelyon 16 dataset [113] consists of 400 Whole Slide Images (WSIs). These samples were taken from two institutions Radboud UMC and UMC Utrecht. The dataset is divided into 270 for training (90 Radboud UMC and 70 UMC Utrecht) and 130 for testing (70 Radboud UMC and 40 and UMC Utrecht).

#### 4.1.3. Biosegmentation Benchmark dataset

The Biosegmentation Benchmark [114], Bio-Image Semantic Query User Environment (BisQue) store the image in the cloud. BisQue is free and open source database. Bisque was designed to facilitate users to share and explore biological images. BisQue[2] dataset comprises of 58 H&E-stained Histopathology Images (HI). The size of images is 896 × 768 including 32 normal and 26 cancerous images.

#### 4.1.4. Tissue Microarray Database

Tissue Microarray (TMA) Database provides TMA design and annotation tool service. TMA also facilitate the researchers with data sharing methods, an image archive, and a publication mechanism. Total number of images present in the "Stanford Tissue Microarray" (TMA)[3] database [115] are 5237 out of which 5044 images reflect different diseases and disorders, and 1524 images are connected to BC. "Breast Carcinoma" appears in the majority of BC images.

#### 4.1.5. Bioimaging 2015 grand challenge dataset

The "Bioimaging" dataset [116] contains 269 Hematoxylin & Eosin (H&E)- stained HI. The images size is 2048 × 1536 pixels taken at 200× magnification. For binary classification, there are two types of images: non-cancerous and malignant. Non-cancerous images are divided into two groups: normal and benign, whereas cancerous images are divided into two groups: "In Situ Carcinoma" and "Invasive Carcinoma". The training dataset has 249 image, including normal (55), benign (69), "In Situ Carcinoma" (63), and "Invasive Carcinoma" (62), and the testing dataset has 20 images, including normal (5), benign (5), "In Situ Carcinoma" (5), and "Invasive Carcinoma" (5).

#### 4.1.6. ICIAR 2018 dataset

ICIAR[4] [117] is an extended version of Bioimaging 2015 breast histology classification challenge dataset, which consists of 400 images in the training dataset distributed as normal (100), benign (100), in situ carcinoma (100), and invasive carcinoma (100), and 100 images in the testing dataset.

#### 4.1.7. Atlas Of Breast Histopathology

The Atlas Of Breast Histopathology dataset [118] provided by the University of Tampere, Finland contains more than 150 images of Histopathology breast cancer. This dataset is a virtual microscopy framework built by researchers where we can see breast tissue on any magnification.

#### 4.1.8. UCI machine learning repository: Breast Cancer Wisconsin diagnostic data set

The Wisconsin Breast Cancer (WBC)[5] dataset [119] contains 569 data samples where 357 samples represent benign and 212 samples represent malignant cases. This dataset contains 11 integer-valued attributes.

#### 4.1.9. MITOS dataset

The MITOS dataset [120] contains approximately 180,000 non-mitotic and 748 non-mitotic Hematoxylin and eosin (H&E) – stained HI. This dataset is provided by MITOS-ATYPIA −14 contest at International Conference on Pattern Recognition (ICPR). The dataset images were scanned by Aperio Scanscope XT and Hamamatsu Nanozoomer 2.0 HT slide scanners in size of 1539 × 1376.

## 5. Deep learning for ultrasound

In this section, our focus is the automatic detection and classification of BC using ultrasound-imaging modality. DL has found its applications in the segmentation and classification of ultrasound BC images. [121] presented the CNN-based "U-Net" [122] architecture (encoder–decoder style neural network) to capture the context and precise localization of lesions. To improve the performance of "U-Net" architecture, [123] designed a CNN architecture based framework for the segmentation and classification of ultrasound breast lesions. The

[2] http://bioimage.ucsb.edu/research/biosegmentation.
[3] http://tma.im/cgi-bin/home.pl.
[4] https://iciar2018-challenge.grand-challenge.org/.
[5] https://www.kaggle.com/uciml/breast-cancer-wisconsin-data.

**Table 6**
Studies conducted for Ultrasound Breast Cancer using Deep Learning Techniques. FE: Feature Extraction, AUC: Area under the Curve; Accu: Accuracy; Sens: Sensitivity; Spec: Specificity, NA:Not Available.

| Related work | Dataset | Input size | Model | Output performance |
|---|---|---|---|---|
| [123] | Dataset:MBUD<br>Total:163<br>Benign:110<br>Malignant:53 | 256 × 256 | FE + ResNet + U-Net | Accu:99.72%, 99.05% |
| [129] | Dataset:private<br>Total:1400 | -NA- | SDAE | Accu: $82.4 \pm 4.5\%$<br>Sens: $0.770 \pm .080$<br>Spec: $0.857 \pm 0.068$ |
| [125] | Dataset:MBUD<br>Total:163<br>Benign:110<br>Malignant:53 | 100 × 100 | CNN | Accu:88.0% |
| [126] | Dataset:OASBUD<br>Total:200<br>Training set: 112<br>Testing set: 40<br>Validation set:48 | -NA- | VGG16 + RPN | Accu:95.0% |

proposed model consists of feature extraction block that includes 6 convolutional layers with a "Batch Normalization" (BN) layer and "ReLu" activation function, "U-Net" architecture, and a modified "ResNet" architecture for classification purpose. This model has potential outcomes in terms of "Dice-Coefficient", "precision", "mean-IOU", "recall", and "accuracy". CNNs have been widely employed for lesion detection in ultrasound images [124]. DL-based models have also been used for the despeckling (denoising) of ultrasound images. CNN has proved to be an effective tool for image despeckling [125], by performing the residual mapping (an accurate estimation of speckles). This approach used two CNNs, one for denoising and the second one for the classification of ultrasound BC images into benign and malignant tumors. Using CNN despeckling, CNN classifier outperformed all classifiers with an accuracy of 88.0%. [126] implemented "Fast Region CNN" (Faster R-CNN) [127] algorithm for the classification of breast lesions. The proposed algorithm has the capability of detecting breast lesions with a bounding box and classifying breast lesions as benign and malignant, in which three independent neural networks were employed for feature extraction, region selection, and classification of these regions. Region Proposal Network (RPN) for region selection has proven to be an efficient tool by decreasing the training and testing time. [128,129] proposed a DL "Autoencoder" based framework, which consists of a "Stacked Denoising Autoencoder" (SDAE) [130] that performs the automatic feature exploration and noise avoidance for the classification of ultrasound breast lesions. This architecture is suitable for small datasets and provides robust breast lesion classification. However, the performance of this framework has been improved by [128], on adding "Intensity Inhomogeneity Correction algorithm" (IICA). Table 6 presents the review work of some studies conducted for BC detection on ultrasound imaging modality.

### 5.1. Datasets for ultrasound

#### 5.1.1. MENDELEY Breast Ultrasound Dataset

MENDELEY Breast Ultrasound Dataset (MBUD) [131] is the imaging dataset collected from UDIAT a Diagnostic Centre of the Sanitaria Parc Tauli, Sabadell Spain with a Siemens ACUSON sequoia C512 system, 17L5 HD linear array transducer (8.5 MHz). This dataset consists of 163 images, out of which 110 are benign and 53 are malignant. This dataset contains four subcategories of malignant including 40 Invasive ductal carcinomas, 4 Ductal carcinomas in situ, 2 invasive Lobular carcinomas, and 7 unspecified lesions. Furthermore, there are three subcategories of benign, which includes 65 unspecified cysts, 39 fibroadenomas, and 6 other different types of benign lesions. The size of each image is 760 × 570 pixels.

**Table 7**
OASBUD fields. ROI: Region of Interest.

| FIELD | DISCRIPTION |
|---|---|
| ID | Identifications of samples. |
| RF1 | 1st scan plane. |
| RF2 | 2nd scan plane. |
| ROI1 | Region of interest of the 1st plane. |
| ROI2 | Region of interest of the 2nd plane. |
| BIRADS | Categories of BI-RADS system. |
| CLASS | 0-benign, 1-malignant. |

#### 5.1.2. Open Access Series of Breast Ultrasound Data

Open Access Series of Breast Ultrasound Data (OASBUD) [126] database consists of raw radio frequency (RF) ultrasound echoes collected in a group of 78 women and each collection has two orthogonal scans. OASBUD database contains 52 malignant and 46 benign breast lesions. The data of each patient has seven fields shown in Table 7

## 6. Deep learning for MRI

Similar to other imaging modalities, Deep Learning in MRI is mostly employed for segmentation, classification and detection of Breast Cancer. However, the significant distinction between MRI and other imaging modalities is the dimensionality. MRI generates 3D scans as opposed to Digital Mammography, Histopathology, and Ultrasound that produce 2D images. Furthermore, MRI sequences also observe variations throughout time. To address these issues, a number of strategies have been developed (as shown in Fig. 15). The most prevalent method is to convert 3D MRI image into 2D images so that conventional 2D Deep Learning models may be employed. This can be accomplished by carving up the 3D_MRI image into 2D_slices/images. Most of the Deep Learning models are designed for RGB images, where the 3 color channels constitute the third dimension. Due to the fact that MRI images are greyscale in nature with just 1 color channel, three 2D_slices can be stacked up and fed as one input image to the model. The resulting opportunity allows for the creation of semi-3D MRI input images with three consecutive slices in a single input image. Other methods involve using whole 3D MRI images, modifying existing 2D DL models to handle 3D data, or using models like "DenseNeT" that were developed particularly to handle 3D imaging data. This section presents the brief over of techniques used for segmentation and classification of Breast Cancer DCE-MRI images. Table 8 demonstrates some studies research conducted for MRI images.

Most of the research studies [136,137,139–141] have implemented U-Net architecture for the detection and segmentation of breast lesion in MRI images. For instance, [139] developed a multi-stage U-Net model obtaining a Dice Similarity Coefficient (DSC) of 72. "Whole

**Table 8**
Studies conducted for Breast Cancer MRI using Deep Learning Techniques. AE: Feature Extraction, AUC: Area under the Curve; Accu: Accuracy; Sens: Sensitivity; Spec: Specificity, NA:Not Available.

| Related work | Dataset | Input size | Model | Output performance |
|---|---|---|---|---|
| [133] | Dataset:private<br>Total:377<br>Benign:267<br>Malignant:110 | NA | AE + Multi-layer Perceptron (MLP) | AUC: $0.8 \pm 10.1$ |
| [134] | Dataset:private<br>Total:703 | -NA- | CNN + LSTM | AUC:0.85 |
| [135] | Dataset1:DCE-MRI<br>Dataset2:DWI<br>Total:72<br>Benign:45<br>Malignant:27 | $40 \times 40 \times 40$ | CNN + LSTM | Accu:84.7% |
| [136] | Dataset:private<br>Total:385<br>Benign: 224<br>Malignant:161 | $39 \times 39 \times 39$ | 3D CNN | $Sens : 0.6429 \pm 0.0537$ |
| [137] | Total:5452 slices | 256 × 256 | U-Net | IOU:76.14% |
| [138] | Dataset:RIDER<br>Total:153<br>Normal: 93<br>Abnormal: 60 | 256 × 256 | SVM + DWT + PCA | Accu:98.03%<br>Sens:0.9642<br>Spec:0.9672 |

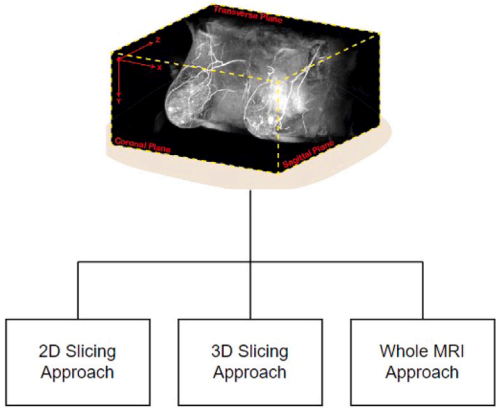


**Fig. 15.** Various approaches for processing 3D_MRI Breast Cancer images using deep learning.
*Source:* Adopted from [132].

Breast mask" (WBM), "Post-Contrast" (PoC) and Subtraction Images were used to create 3 RGB channels. As an alternative, [140] obtained a DSC score of 61 for breast lesion segmentation. To get a DSC of 0.865, [141] utilized the U-Net segmentation model by combining 4 different MRI sequences, including "T1-weighted" (T1-W), "T2-weighted" (T2-W), "Diffusion Weighted" (DW), and "DCE-MRI". In some research studies [142–144], the authors obtained the DSC between 96 and 99. The BC detection relies heavily on the precise segmentation of 3D_MRI data. A novel 3D Automatic Levels Propagation Approach (3D-ALPA), that enables both multi-planer and multi-tumor segmentation was proposed by [145] for the automatic segmentation of 3D_MRI. Deep Learning models have also employed for the segmentation of fibroglandular tissue (FGT), making it possible to determine the Mammographic density automatically [146–148]. In a research study [132], single Deep Learning model has been implemented for lesion, breast and FGT segmentation, after which a conventional Machine Learning algorithm has been used for lesion classification. The proposed model achieved an AUC value of 0.90 for classification task and a DSC score of 0.89 for segmentation task.

It is crucial to remember that majority of the aforementioned segmentation techniques utilize the Whole Breast Mask (WBM). When applied to an MRI image, these breast masks allow only the pixels associated with the breasts to pass through, while changing the values of all other pixels to zero. These masks have two primary functions: (i) They can direct the Deep Learning models to focus on the appropriate location for segmentation and detection. (ii) These WBM's can also be utilized to determine the "Mammographic" density, a crucial sign of a higher risk of BC.

Dynamic Contrast-Enhanced MRI (DCE-MRI) is an essential element of a clinical breast MRI screening protocol. DCE-MRI contains morphological as well as contrast dynamics, which are important in image interpretation and has been proven to be very crucial in the diagnosis of Breast Cancer [149–151]. Deep Learning-based CNN models applied by [133,138,152] for the BC diagnosis on MRI images are similar to Mammography, Histopathology, and ultrasound 2D images, but field experts always review MRI images with temporal 3D image sequences. Unsupervised learning technique RNN, which can recall previous sequences and deal with the features extracted from Breast Cancer MRI images using CNN architecture is shown in Fig. 16. "Long-Short-Term-Memory" (LSTM) [153] is an advanced method of RNN including "input", "forgetting gate", and "output gate" that learns the information a long time ago [134]. Applied "LSTM" model on the sequence of features extracted by "VGG" model from MRI breast images and has given an AUC of 0.85. Breast tumor segmentation is an important step for BC diagnosis [135]. Proposed a CNN-RNN based architecture for benign and malignant image classification by utilizing DCE-MRI and Diffusion Weighted Imaging (DWI) MRI. For balancing huge parameters, a dense block has been added in the "RNN-CNN" unit. RNN has proved to be an effective model in MRI sequences for BC classification and therefore, can be used for other Breast Cancer applications.

### 6.1. Datasets for MRI

#### 6.1.1. QIN breast DCE-MRI

Breast DCE-MRI [137] dataset contains Dynamic Contrast-Enhanced Magnetic Resonance Imaging (DCE-MRI), which were collected using Siemens 3T TIM Trio system. Images were collected at four-time points: (1) before treatment, (2) after the first cycle of treatment (3) in the middle of treatment (4) after completion of treatment before surgery.

#### 6.1.2. Reference Image Database to Evaluate Response breast MRI

Reference Image Database to Evaluate Response (RIDER) [154] is a collection of DCE-MRI breast images collected from 5 subjects, generally employed for the evaluation of breast MRI segmentation techniques. The database contains the 2 MRI scans for each subject. National Cancer Institute of the United States is the copyright holder

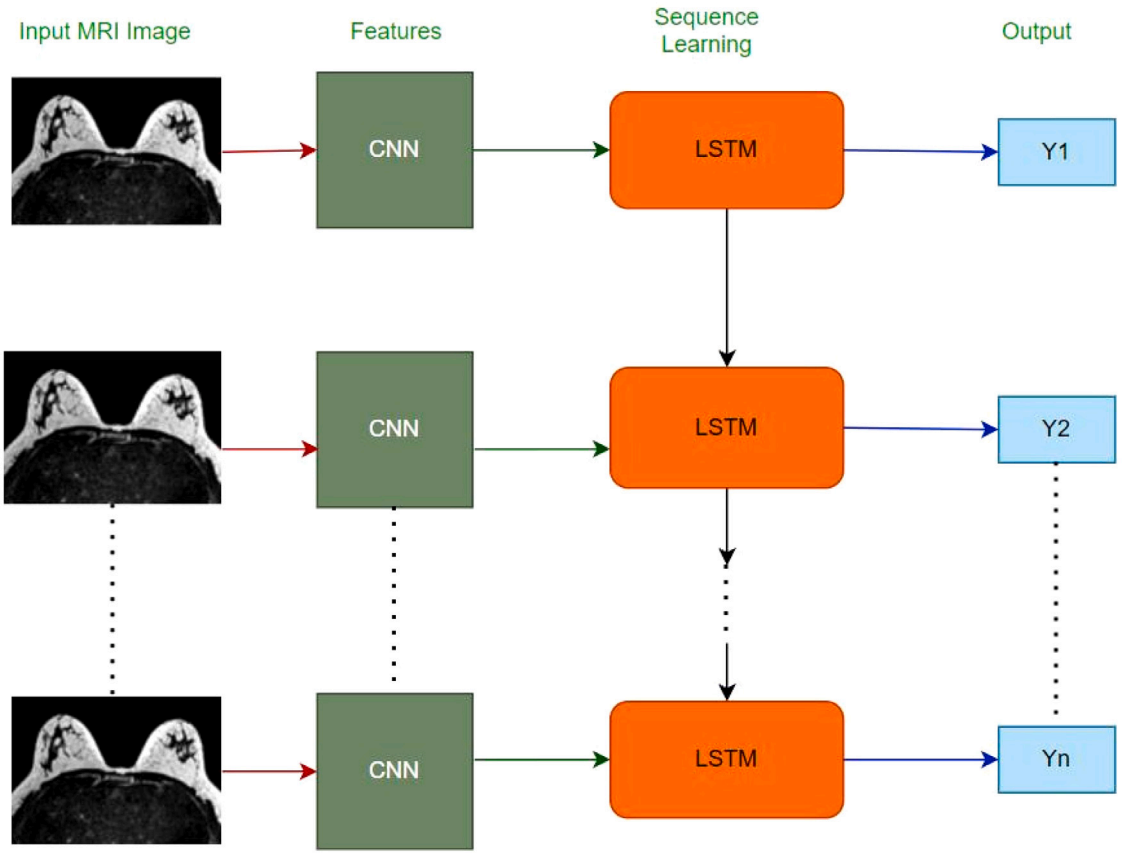


**Fig. 16.** CNN-RNN architecture for Breast Cancer classification Using MRI.

of this dataset, but it is still available in free and can be downloaded from the[6] Cancer Imaging Archive.

## 7. Deep learning for Nuclear Medicine Imaging

Nuclear Medicine Imaging (NMI) including PET/CT scans have the ability to precisely stage Whole Body (WB) meta-static disease and evaluate therapy response [155,156], which had a tremendous impact and has enabled Breast Cancer patients to get care that is more personalized to their specific needs. PET/CT scans are more effective in identifying distant metastasis due to their high sensitivity and specificity and therefore, these techniques are not well suited for resolving the axillary nodal regions or small breast lesions [157]. Furthermore, PET/CT scans are less suitable for early diagnosis of BC as compared to the above mentioned imaging modalities. However, NMI techniques have been useful for identification, classification and segmentation of axillary lymph nodes. So it should come as no surprise that Deep Learning is also being marginally applied in NMI context. In some research work conducted by [158], a CNN model has been able to precisely identify and segment lesions in WB PET/CT scans of BC patients after being trained to collect the Metabolic Tumor Volume (MTV) for lymphoma and lung cancer patients. The statistically significant correlation was found between manually derived MTV and Deep Learning, demonstrating the generalizability of Deep Neural Network Learning models.

BC is the leading cause of bone metastasis among women. In consideration of this, [159] proposed a sophisticated CNN model for identifying BC metastasis using WB scintigraphy scans. WB scans were classified as either benign or malignant with a classification result of 92.5%. For the purpose of assisting clinicians in the detection of axillary lymph node metastasis by utilizing PET/CT scans, a 3D CNN model has been developed by [158]. In an another research study [160], DCNN model has been implemented to predict the pathological responses of patients with metastasis Breast Cancer by employing PET/CT scans. The predicted outcomes were compared with the conventional methods (MTV, "maxi- mum standardized uptake value" (MSPV)), the results demonstrated that the DCNN model produced better AUC values than the conventional indicators. [161] developed a Deep Learning Signatures for predicting Sentinel Lymph Node (SLN) Status (metastasis or non-metastasis) and differentiating the number of metastatic SLN (1–2 or more than 2) using breast cancer CT images pre-operatively and non-invasively.

## 8. Deep learning for thermal imaging

Thermography is a painless and low cost medical imaging modality used for early detection of BC. Deep Learning (DL) models have also been utilized for segmentation and classification of thermal images. Segmentation is a very challenging task for disease diagnosis. Accurate segmentation of medical images can improve the diagnostic performance. A two stage novel segmentation model has been proposed by [162] to improve the BC diagnosis. The proposed model uses the amalgamation of "Gaussian Mean Shift" (GMS) and "roulette wheel" methods for segmentation process. The Designed segmentation method provides the Jaccard index (JI) of 91.81%, Dice coefficient (DC) of 84.86%, and Hausdorff distance (HD) of 4.87, respectively. Another framework has been presented by [163] for the segmentation of Thermographic images to enhance the accuracy of BC diagnosis. Here, "Canny Edge Detector" has been employed for edge detection that uses Gaussian function for image smoothing and "Hough transform" to detect the boundaries of the lower breast, respectively.

[6] www.cancerimagingarchive.net.

In an another study, a DL based approach proposed by [164] employs four CNN architectures including "VGG-16", "VGG-19", "ResNet50", and "Inception-V3" for binary classification of BC using thermal imaging on "Dataset for Mastology Research Infra-Red" (DMR-IR) dataset. "ResNet50" has shown the highest performance with an accuracy of 88.90%. A five (5) step methodology namely "Data Acquisition", "Image Pre-Processing", "Segmentation", "Feature Extraction", and "Classification" has been adopted by [165] for BC detection from thermal images. CNNs employed for the classification task achieved a validation accuracy of 97.91%. After that CNN model parameters has been optimized by the Bayes Optimization algorithm to achieve an accuracy of 98.95%. [166] employed pre-trained state-of-art CNN model "Inception-V3" for the classification of BC thermal images. Some pre-processing operations including sharpening filter and "Contrast Limited Adapt Histogram Equalization" (CLAHE) have been used to increase the contrast of images and for intensity normalization, respectively to the whole training dataset. The model gives an accuracy of 80% and a recall rate of 83.33%. [167] proposed a simple CNN framework for Breast Cancer detection on the DMR-IR dataset. The authors compared the state-of-art deep CNN architectures including "ResNet", "SeResNet", "VGG16", "Inception", "InceptionResNetV2", and "Xception" with the proposed CNN model and the results demonstrate that the simpler CNN model outperformed deeper CNN architectures. Here, the Hyper-Parameter Bayesian Optimization with "ree Parzen Estimator" (TPE) has been applied to design optimal CNN architecture. A multi-input CNN based framework has been designed by [168] for the classification of thermal images. The authors merged the different views of thermals images with clinical and personal data of patients to detect the BC at an early stage. optimal feature selection is very crucial for the precise diagnosis of diseases. In a research study conducted by [169], a two stage architecture has been developed, which consists of "VGG16" for feature extraction and "Dragonfly" algorithm for optimal selection of features, respectively. The proposed approach has been evaluated on DMR-IR dataset which demonstrates an accuracy of 100%. In an another research analysis [170], various DL models including InceptionV3, InceptionV4 and MV4 (a modified version of InceptionV4 which maintains the computational cost across the layers of network) have been experimented on DMR-IR to diagnose the BC from thermal images.

From our study, we concluded that CNN-based models have achieved promising results in medical imaging application for BC diagnosis. However, CNN models have not been widely used for thermal images. Table 9 represents the brief overview of research study conducted for thermography imaging modality.

### 8.1. Datasets for breast thermography

#### 8.1.1. Dataset for Mastology Research with Infrared Image

Dataset for Mastology Research with Infrared Image (DMR-IR)[7] [171] is an open-access database of mastological images used for early detection of Breast Cancer. This database provided by Federal Fluminense University contains IR images, digitalized mammograms, and stores the information of patients such as medical history, eating habits, age, symptoms, etc. In addition to IR images, this group also acquires Ultrasound and MRI images. The images were captured with FLIR-SC 620 imaging camera with both static and dynamic protocols. Each Infrared image has dimensions 640 × 480.

[7] http://visual.ic.uff.br/dmi/.

## 9. Deep Reinforcement Learning for breast cancer diagnosis

Deep Reinforcement Learning (DRL)is the amalgamation of DL architectures and Reinforcement Learning (RL) algorithms to produce efficient algorithms that can be used to solve problems in robotic engineering, healthcare maintenance, gaming applications, financing, etc. In medical imaging, DRL can be used for landmark detection, image registration, lesion localization, and detection view plane localization, etc. DRL has been very less explored in BC diagnosis. A novel technique based on DRL framework has been presented by [172] for breast lesion detection utilizing DCE-MRI breast images. The proposed approach significantly mitigates the lesion detection inference time. Designing of algorithms that can balance the early detection of BC with the cost of over-screening is the utmost need. In a research study conducted by [173], a RL framework has been employed for the early detection of BC using Mammogram BC images.

## 10. Future directions and challenges

This section discusses the future scope for the research that can be employed for the BC diagnosis. Despite the success achieved by DL models, there are some challenges and limitations about DL that are needed to overcome for BC detection and classification. The key challenges identified throughout our study are discussed below:

- The major challenge is the lack of a comprehensive dataset for training the DL algorithms for medical imaging. DL models are data-hungry because the efficacy of these models depends on the size and quality of training datasets. Moreover, creating a large dataset is also a difficult task because annotating medical images is laborious, time-consuming and requires many efforts to oust human error.
- Another most important challenge is unsupervised learning for BC classification. Most of the studies use supervised learning for the classification of breast cancer images. Although supervised Learning-based models have led to better results, in practice, it is very difficult to get annotated breast images by professional doctors. In reality, most of the breast images available are unlabeled. Therefore, there is a desperate need for unsupervised Learning-based models for the classification of BC images.
- Another limitation is that most of the researchers used clinical datasets (private data- sets) for evaluation and analysis purposes. Therefore, comparing the performance of such models across research is challenging.
- Furthermore, some studies used data augmentation techniques rather than transfer learning to avoid overfitting. There are very few pre-trained models in the field of medical imaging. Although "ImageNet" pre-trained models can be applied to various medical imaging modalities, the amount of improvement achieved from these pre-trained ImageNet models is not that great. Therefore, there is a great need for those approaches that work better but does not require a huge amount of data.
- The class imbalanced problem is a serious challenge for DL models. The results could be biased towards the majority class. Many BC imaging datasets are imbalanced e.g., BreakHis dataset has an imbalanced ratio of 0.45 at image level and 0.41 at patient level. The imbalanced distribution is also present in multiclass problem both at patient and image level. Therefore, another problem that need to be addressed is the lack of balanced datasets.
- Medical data privacy-preserving poses another important challenge for Machine Learning and Deep Learning algorithms like Deep Convolution networks that require huge training data. Due to privacy regulations, it becomes difficult to share the data in a central repository. Therefore, collaborative and decentralized training of Deep Convolution Neural Networks (DCNN) can be performed without sharing patient data.

**Table 9**
Studies conducted for BC detection using thermal images. CONV:"Convolutional Layer"; POOL:"Pooling"; FC: "Fully-Connected Layer"; AUC:"Area Under Curve"; ROC:"Receiver Operating Curve"; Accu:"Accuracy"; Sens:"Sensitivity"; Spec:"Specificity".

| References | Dataset | Input size | Models | Results |
|---|---|---|---|---|
| [165] | Total:3895<br>Benign:3098<br>Malignant:797 | 640 × 480 | CNN | Accu:98.95% |
| [166] | Dataset:DMR-IR<br>Total:40<br>Benign:18<br>Malignant:22 | 229 × 229 | InceptionV3 | Accu:80%<br>Recall rate:83.33% |
| [164] | Dataset:DMR-IR<br>Total:144<br>Healthy:88<br>Suspicious:56 | 224 × 224 | VGG16+VGG19+<br>InceptionV3+<br>ResNet50 | Accu for<br>ResNet50:88.9% |
| [167] | Dataset:DMR-IR<br>Total:144<br>Healthy:88<br>Unhealthy:56 | 250 × 300 | CNN + TPE | Accu:86%<br>Sens:0.90<br>AUC:0.85 |
| [168] | Dataset:DMR-IR<br>Total:144<br>Healthy:88<br>Unhealthy:56 | 250 × 300 | CNN + TPE | Accu:86%<br>Sens:90<br>AUC:0.85 |
| [162] | Not Available | Not Available | GMS + Roulette Wheel | JI:91.81%<br>DC:84.86%<br>HD:4.87 |
| [170] | Dataset:DMR-IR<br>Total:287 people<br>Sick:48<br>Healthy:239 | 229 × 229 | InceptionV3 +<br>InceptionV4 +<br>MV4 | Accu of<br>InceptionV4:99.712%<br>Accu of MV4: 99.748% |

- Another challenge in medical image analysis is the robustness issue of data collection methods, which can be solved by using different scanners for image acquisition, different views and sizes of various imaging modalities, different lighting conditions, different color presentation, and enlargement factors. Using such differences more data can be introduced slowly.
- There are currently just a handful of DL models that combine non-imaging characteristics (cancer history, genetic information) with imaging data. Many such models must be developed that combine radiomic characteristics with the image data.
- Label noise also poses a serious challenge for Deep Learning models. During the course of cancer development, BC spreads from one region to another region in breast issue. As a result, different parts of the same breast tissue may have different stages of BC, resulting in multiple sub-category annotations for the same image. These images can confuse the DL in multi-classification problem.
- Deep Reinforcement Learning (DRL), a sophisticated and emerging technology is an open research area and has not been fully explored for Medical Image Analysis.
- Artificial intelligence (AI) has great potential to accelerate scientific discovery in medicine and to transform healthcare. Ethical, medicolegal and regulatory issues are the challenging aspects of this new technology [174]. These are particularly important for standalone AI tools that independently make decisions on Breast Cancer images without human intervenion. Due to AI algorithms "black-box" nature, there is often a lack of transparency in decision-making. Therefore, all hidden pathways of algorithm-made decisions would not be fully comprehended by its users. When an AI system makes an error, who will be, therefore, responsible for the unwanted outcomes?. Therefore, Standard regulations should be developed along with the new technology to make AI a reality.
- Aspects, such as data bias, algorithmic bias and performance drift for adaptive algorithms also raises ethical concerns. The risk for biases should be considered when deciding which DL technology to use to train the algorithms and which datasets (considering their quality and diversity) to use for the training.

## 11. Discussion

Breast Cancer cases are rising at an alarming rate all over the world. Death rates in developed countries are significantly higher and they are rising in every region of the world. Early detection and diagnosis of BC is critical in improving long-term survivability. Medical Image Analysis (MIA) using CAD has proven to be the most effective approach for the early diagnosis of BC and treatment. The usage of DL models for Breast Cancer diagnosis greatly assists doctors in making a final decision. Deep Learning do not require feature extraction methods explicitly, as they learn the low-level, middle-level and high-level features automatically. Based on the severity of BC, a greater number of publications have been published. As a result, compiling all research studies using DL approaches into a single article is a difficult process. However, this study provides a systematic approach, attempting to cover the existing BC databases, segmentation techniques, current findings on classification and detection of BC. Our research study suggests that Mammography and Histopathology are two common imaging modalities employed for the analysis of Breast Cancer, and our literature also reveal that Mammography is an effective technique for early detection of BC. However, Mammogram images have limited contrast, therefore different noise removal and contrast enhancement techniques are employed during the pre-processing phase. Some studies have also shown that false positive and false negative classification rate reduces when pre-processing and data augmentation techniques are implemented on BC images. Majority of Mammography research focuses on calcification and mass detection. Researchers could use CNN-based algorithms to improve density classification and asymmetry detection and classification, which have fewer related publications. Most of the DL models are trained on freely available datasets. However, the size and quality of these datasets have a great impact on the performance of these systems. Training DL models over these datasets could improve their performance. Furthermore, from our study, it is found that the improvement of DL models for limited medical image datasets is an open research challenge. Most authors, however, have used, Transfer Learning, data augmentation and regularization strategies to avert over-fitting and elevate model performance for limited datasets. Deep Learning in Combination with hand-engineered feature extraction methods also provided better results. The combined approach of supervised and unsupervised learning

is applied on MRI images to improve classification results. However, when compared to 2D imaging data, automatic identification of Breast Cancer using 3D imaging is more challenging. Because 3D datasets are more informative than 2D datasets, new strategies must be created to produce higher accuracy results using these 3D datasets. Our research study also reveal that, Mammography and Histopathology imaging modalities have enormous datasets in the range of thousands of patients from various medical centres. MRI modality rarely exceed 500 patients and are often from a single site. The size of ultrasound imaging modality datasets is in the middle of the other two modalities, with tens of thousands of patients. This, of course, benefits AI performance in Mammography and Histopathology studies, as larger datasets and data from several sources often result in higher performance and generalization of DL models. Therefore, larger and diverse MRI, ultrasound datasets need to be generated to evaluate the already existing methods for larger datasets.

There are two key issues that must be addressed when adopting DL approaches to diagnose Breast Cancer: how to detect BC at an early stage and how to leverage a high accuracy rate. For a Deep Learning model to guarantee 100% accuracy, large datasets are necessary. As a result, the availability of comprehensive dataset is crucial to enable the efficacy of AI based Deep Learning techniques in segmentation, classification, and detection of BC. Pre-screening exams can be performed using the Breast Self-Examination (BSE) approach to enable early detection. Therefore, Deep Learning algorithm should be efficient (light-weighted) with its resources so that a self-screening application can be installed on a portable device. We suggest future work to consider producing a representative dataset, putting together segmentation and augmentation methods, and developing light-weighted DL models.

## 12. Conclusion

Earlier detection of Breast Cancer can improve the survival rate of patients. Fortunately, advancements in medical imaging techniques have made it possible to diagnose Breast Cancer at an early stage. The rapid development of Artificial Intelligence based techniques in Medical Image Analysis (MIA) have made it possible to fully utilize large datasets for improved BC diagnosis and precision medicine by automatically extracting the relevant features. In this research study, we reviewed the most recent research on the subject of applying ML, DL and Deep Reinforcement Learning on several medical imaging modalities for Breast Cancer diagnosis. Even if there have been a lot of meaningful and effective algorithms produced so far, there is still a lack of consistency that each algorithm is facing in some way or another. This research study explores a variety of Breast Cancer medical imaging techniques, such as "Mammography", "Magnetic Resonance Imaging (MRI)", "Histopathology", "Ultrasound (US)", "Nuclear Medicine Imaging (NMI)", and "Thermography", in order to systematically review the benefits, drawbacks, and efficacy of recent Machine Learning, Deep Learning, and Deep Reinforcement Learning techniques. This exploration covers everything from detection to segmentation, as well as classification and the generation of images. This study also provides a concise discussion of the several datasets that are accessible for each imaging technique. Furthermore, this research study suggests future research areas and challenges in choosing the Artificial Intelligence methods for BC diagnosis utilizing different medical imaging modalities. According to the aforementioned analysis, there is a strong requirement for a unified, fully-automatic framework that is able to effectively diagnose Breast Cancer with minimal effort.

## Declaration of competing interest

The authors declare that they have no known competing financial interests or personal relationships that could have appeared to influence the work reported in this paper.

## Acknowledgments

This work was supported by the Technical Education Quality Improvement Programme (TEQIP-III) of Government of India project (Grant No. IUST/TEQIP/19/36-53).

## References

[1] C.H. Lee, D.D. Dershaw, D. Kopans, P. Evans, B. Monsees, D. Monticciolo, R.J. Brenner, L. Bassett, W. Berg, S. Feig, et al., Breast cancer screening with imaging: recommendations from the Society of Breast Imaging and the ACR on the use of mammography, breast MRI, breast ultrasound, and other technologies for the detection of clinically occult breast cancer, J. Am. Coll. Radiol. 7 (1) (2010) 18–27.

[2] J. Tang, R.M. Rangayyan, J. Xu, I. El Naqa, Y. Yang, Computer-aided detection and diagnosis of breast cancer with mammography: recent advances, IEEE Trans. Inf. Technol. Biomed. 13 (2) (2009) 236–251.

[3] K. Horsch, M.L. Giger, C.J. Vyborny, L. Lan, E.B. Mendelson, R.E. Hendrick, Classification of breast lesions with multimodality computer-aided diagnosis: observer study results on an independent clinical data set, Radiology 240 (2) (2006) 357–368.

[4] S. Malur, S. Wurdinger, A. Moritz, W. Michels, A. Schneider, Comparison of written reports of mammography, sonography and magnetic resonance mammography for preoperative evaluation of breast lesions, with special emphasis on magnetic resonance mammography, Breast Cancer Res. 3 (1) (2000) 1–6.

[5] L. Tabár, B. Vitak, H.-H.T. Chen, M.-F. Yen, S.W. Duffy, R.A. Smith, Beyond randomized controlled trials: organized mammographic screening substantially reduces breast carcinoma mortality, Cancer: Interdiscip. Int. J. Am. Cancer Soc. 91 (9) (2001) 1724–1731.

[6] D.B. Kopans, Sonography should not be used for breast cancer screening until its efficacy has been proven scientifically, Am. J. Roentgenol. 182 (2) (2004) 489–491.

[7] C. Dromain, C. Balleyguier, Contrast-enhanced digital mammography, in: Digital Mammography, Springer, 2010, pp. 187–198.

[8] K.M. Kelly, J. Dean, W.S. Comulada, S.-J. Lee, Breast cancer detection using automated whole breast ultrasound and mammography in radiographically dense breasts, Eur. Radiol. 20 (3) (2010) 734–742.

[9] V. Corsetti, N. Houssami, M. Ghirardi, A. Ferrari, M. Speziani, S. Bellarosa, G. Remida, C. Gasparotti, E. Galligioni, S. Ciatto, Evidence of the effect of adjunct ultrasound screening in women with mammography-negative dense breasts: interval breast cancers at 1 year follow-up, Eur. J. Cancer 47 (7) (2011) 1021–1026.

[10] D. Truhn, S. Schrading, C. Haarburger, H. Schneider, D. Merhof, C. Kuhl, Radiomic versus convolutional neural networks analysis for classification of contrast-enhancing lesions at multiparametric breast MRI, Radiology 290 (2) (2019) 290–297.

[11] E. Honda, R. Nakayama, H. Koyama, A. Yamashita, Computer-aided diagnosis scheme for distinguishing between benign and malignant masses in breast DCE-MRI, J. Digit. Imaging 29 (3) (2016) 388–393.

[12] X. Yang, L. Wu, W. Ye, K. Zhao, Y. Wang, W. Liu, J. Li, H. Li, Z. Liu, C. Liang, Deep learning signature based on staging CT for preoperative prediction of sentinel lymph node metastasis in breast cancer, Acad. Radiol. 27 (9) (2020) 1226–1233.

[13] Z. Han, B. Wei, Y. Zheng, Y. Yin, K. Li, S. Li, Breast cancer multi-classification from histopathological images with structured deep learning model, Sci. Rep. 7 (1) (2017) 1–10.

[14] M. Frize, C. Herry, R. Roberge, Processing of thermal images to detect breast cancer: Comparison with previous work, in: Proceedings of the Second Joint 24th Annual Conference and the Annual Fall Meeting of the Biomedical Engineering Society][Engineering in Medicine and Biology, Vol. 2, IEEE, 2002, pp. 1159–1160.

[15] E.Y.K. Ng, L.N. Ung, F.C. Ng, L.S.J. Sim, Statistical analysis of healthy and malignant breast thermography, J. Med. Eng. Technol. 25 (6) (2001) 253–263.

[16] M.A. Farooq, P. Corcoran, Infrared imaging for human thermography and breast tumor classification using thermal images, in: 2020 31st Irish Signals and Systems Conference, ISSC, IEEE, 2020, pp. 1–6.

[17] M. Veta, J.P. Pluim, P.J. Van Diest, M.A. Viergever, Breast cancer histopathology image analysis: A review, IEEE Trans. Biomed. Eng. 61 (5) (2014) 1400–1411, http://dx.doi.org/10.1109/TBME.2014.2303852.

[18] C. Lehman, R. Wellman, D. Buist, K. Kerlikowske, A. Tosteson, D. Miglioretti, et al., Diagnostic accuracy of digital screening mammography with and without computer-aided detection, JAMA Internal Med. 175 (11) (2015) 1828–1837.

[19] R.R. Schaller, Moore's law: past, present and future, IEEE Spectr. 34 (6) (1997) 52–59.

[20] E.J. Topol, High-performance medicine: the convergence of human and artificial intelligence, Nat. Med. 25 (1) (2019) 44–56, http://dx.doi.org/10.1038/s41591-018-0300-7.

[21] A. Esteva, A. Robicquet, B. Ramsundar, V. Kuleshov, M. DePristo, K. Chou, C. Cui, G. Corrado, S. Thrun, J. Dean, A guide to deep learning in healthcare, Nat. Med. 25 (1) (2019) 24–29, http://dx.doi.org/10.1038/s41591-018-0316-z.

[22] J.V. Tu, Advantages and disadvantages of using artificial neural networks versus logistic regression for predicting medical outcomes, J. Clin. Epidemiol. 49 (11) (1996) 1225–1231, http://dx.doi.org/10.1016/S0895-4356(96)00002-9.

[23] C. Amrit, T. Paauw, R. Aly, M. Lavric, Identifying child abuse through text mining and machine learning, Expert Syst. Appl. 88 (2017) 402–418, http://dx.doi.org/10.1016/j.eswa.2017.06.035.

[24] M. Crawford, T.M. Khoshgoftaar, J.D. Prusa, A.N. Richter, H. Al Najada, Survey of review spam detection using machine learning techniques, J. Big Data 2 (1) (2015) 1–24, http://dx.doi.org/10.1186/s40537-015-0029-9.

[25] Y. Deldjoo, M. Elahi, P. Cremonesi, F. Garzotto, P. Piazzolla, M. Quadrana, Content-based video recommendation system based on stylistic visual features, J. Data Semant. 5 (2) (2016) 99–113.

[26] K. Al-Dulaimi, V. Chandran, K. Nguyen, J. Banks, I. Tomeo-Reyes, Benchmarking HEp-2 specimen cells classification using linear discriminant analysis on higher order spectra features of cell shape, Pattern Recognit. Lett. 125 (2019) 534–541, http://dx.doi.org/10.1016/j.patrec.2019.06.020.

[27] W. Liu, Z. Wang, X. Liu, N. Zeng, Y. Liu, F.E. Alsaadi, A survey of deep neural network architectures and their applications, Neurocomputing 234 (2017) 11–26, http://dx.doi.org/10.1016/j.neucom.2016.12.038.

[28] S. Pouyanfar, S. Sadiq, Y. Yan, H. Tian, Y. Tao, M.P. Reyes, M.-L. Shyu, S.-C. Chen, S.S. Iyengar, A survey on deep learning: Algorithms, techniques, and applications, ACM Comput. Surv. 51 (5) (2018) 1–36, http://dx.doi.org/10.1145/3234150.

[29] M.Z. Alom, T.M. Taha, C. Yakopcic, S. Westberg, P. Sidike, M.S. Nasrin, M. Hasan, B.C. Van Essen, A.A. Awwal, V.K. Asari, A state-of-the-art survey on deep learning theory and architectures, Electronics 8 (3) (2019) 292, http://dx.doi.org/10.3390/electronics8030292.

[30] Y. LeCun, Y. Bengio, G. Hinton, Deep learning, Nature 521 (7553) (2015) 436–444.

[31] Z. Jiao, X. Gao, Y. Wang, J. Li, A deep feature based framework for breast masses classification, Neurocomputing 197 (2016) 221–231.

[32] G. Chartrand, P.M. Cheng, E. Vorontsov, M. Drozdzal, S. Turcotte, C.J. Pal, S. Kadoury, A. Tang, Deep learning: a primer for radiologists, Radiographics 37 (7) (2017) 2113–2131.

[33] D. Komura, S. Ishikawa, Machine learning approaches for pathologic diagnosis, Virchows Archiv 475 (2) (2019) 131–138, http://dx.doi.org/10.1007/s00428-019-02594-w.

[34] C. Li, D. Xue, Z. Hu, H. Chen, Y. Yao, Y. Zhang, M. Li, Q. Wang, N. Xu, A survey for breast histopathology image analysis using classical and deep neural networks, in: International Conference on Information Technologies in Biomedicine, Springer, 2019, pp. 222–233, http://dx.doi.org/10.1007/978-3-030-23762-2_20.

[35] D. Wang, A. Khosla, R. Gargeya, H. Irshad, A.H. Beck, Deep learning for identifying metastatic breast cancer, 2016, arXiv preprint arXiv:1606.05718.

[36] Ş. Öztürk, B. Akdemir, A convolutional neural network model for semantic segmentation of mitotic events in microscopy images, Neural Comput. Appl. 31 (8) (2019) 3719–3728, http://dx.doi.org/10.1007/s00521-017-3333-9.

[37] H. Yu, L.T. Yang, Q. Zhang, D. Armstrong, M.J. Deen, Convolutional neural networks for medical image analysis: state-of-the-art, comparisons, improvement and perspectives, Neurocomputing 444 (2021) 92–110.

[38] W. Fang, P.E. Love, H. Luo, L. Ding, Computer vision for behaviour-based safety in construction: A review and future directions, Adv. Eng. Inform. 43 (2020) 100980, http://dx.doi.org/10.1016/j.aei.2019.100980.

[39] H.-C. Li, Z.-Y. Deng, H.-H. Chiang, Lightweight and resource-constrained learning network for face recognition with performance optimization, Sensors 20 (21) (2020) 6114, http://dx.doi.org/10.3390/s20216114.

[40] W. Wang, J. Gang, Application of convolutional neural network in natural language processing, in: 2018 International Conference on Information Systems and Computer Aided Education, ICISCAE, IEEE, 2018, pp. 64–70, http://dx.doi.org/10.1109/ICISCAE.2018.8666928.

[41] D. Palaz, M. Magimai-Doss, R. Collobert, End-to-end acoustic modeling using convolutional neural networks for HMM-based automatic speech recognition, Speech Commun. 108 (2019) 15–32, http://dx.doi.org/10.1016/j.specom.2019.01.004.

[42] I. Goodfellow, Y. Bengio, A. Courville, Deep Learning, MIT Press, 2016.

[43] Y. LeCun, L. Bottou, Y. Bengio, P. Haffner, Gradient-based learning applied to document recognition, Proc. IEEE 86 (11) (1998) 2278–2324.

[44] A. Krizhevsky, I. Sutskever, G.E. Hinton, Imagenet classification with deep convolutional neural networks, Adv. Neural Inf. Process. Syst. 25 (2012).

[45] K. Simonyan, A. Zisserman, Very deep convolutional networks for large-scale image recognition, 2014, arXiv preprint arXiv:1409.1556.

[46] K. He, X. Zhang, S. Ren, J. Sun, Deep residual learning for image recognition, in: Proceedings of the IEEE Conference on Computer Vision and Pattern Recognition, CVPR, 2016, pp. 223–226.

[47] P. Ballester, R.M. Araujo, On the performance of GoogLeNet and AlexNet applied to sketches, in: Thirtieth AAAI Conference on Artificial Intelligence, 2016, pp. 22–26.

[48] J. Deng, W. Dong, R. Socher, L.-J. Li, K. Li, L. Fei-Fei, Imagenet: A large-scale hierarchical image database, in: 2009 IEEE Conference on Computer Vision and Pattern Recognition, Ieee, 2009, pp. 248–255, http://dx.doi.org/10.1109/CVPR.2009.5206848.

[49] C. Szegedy, W. Liu, Y. Jia, P. Sermanet, S. Reed, D. Anguelov, D. Erhan, V. Vanhoucke, A. Rabinovich, Going deeper with convolutions, in: Proceedings of the IEEE Conference on Computer Vision and Pattern Recognition, 2015, pp. 1–9.

[50] C. Szegedy, V. Vanhoucke, S. Ioffe, J. Shlens, Z. Wojna, Rethinking the inception architecture for computer vision, in: Proceedings of the IEEE Conference on Computer Vision and Pattern Recognition, 2016, pp. 2818–2826.

[51] C. Szegedy, S. Ioffe, V. Vanhoucke, A.A. Alemi, Inception-v4, inception-resnet and the impact of residual connections on learning, in: Thirty-First AAAI Conference on Artificial Intelligence, 2017, pp. 34–40.

[52] F. Chollet, Xception: Deep learning with depthwise separable convolutions, in: Proceedings of the IEEE Conference on Computer Vision and Pattern Recognition, 2017, pp. 1251–1258.

[53] R.J. Williams, D. Zipser, A learning algorithm for continually running fully recurrent neural networks, Neural Comput. 1 (2) (1989) 270–280.

[54] A. Ng, et al., Sparse autoencoder, CS294A Lect. Notes 72 (2011) (2011) 1–19.

[55] I. Goodfellow, J. Pouget-Abadie, M. Mirza, B. Xu, D. Warde-Farley, S. Ozair, A. Courville, Y. Bengio, Generative adversarial nets, Adv. Neural Inf. Process. Syst. 27 (2014).

[56] R.S. Sutton, A.G. Barto, Reinforcement Learning: An Introduction, MIT Press, 2018.

[57] V. Mnih, K. Kavukcuoglu, D. Silver, A. Graves, I. Antonoglou, D. Wierstra, M. Riedmiller, Playing atari with deep reinforcement learning, 2013, arXiv preprint arXiv:1312.5602.

[58] A. Bernstein, E. Burnaev, Reinforcement learning in computer vision, in: Tenth International Conference on Machine Vision (ICMV 2017), Vol. 10696, SPIE, 2018, pp. 458–464.

[59] C. Finn, X.Y. Tan, Y. Duan, T. Darrell, S. Levine, P. Abbeel, Deep spatial autoencoders for visuomotor learning, in: 2016 IEEE International Conference on Robotics and Automation, ICRA, IEEE, 2016, pp. 512–519.

[60] J. Luketina, N. Nardelli, G. Farquhar, J. Foerster, J. Andreas, E. Grefenstette, S. Whiteson, T. Rocktäschel, A survey of reinforcement learning informed by natural language, 2019, arXiv preprint arXiv:1906.03926.

[61] M. Zhang, J. Xu, E. Abaci Turk, P.E. Grant, P. Golland, E. Adalsteinsson, Enhanced detection of fetal pose in 3d mri by deep reinforcement learning with physical structure priors on anatomy, in: International Conference on Medical Image Computing and Computer-Assisted Intervention, Springer, 2020, pp. 396–405.

[62] R. Liao, S. Miao, P. de Tournemire, S. Grbic, A. Kamen, T. Mansi, D. Comaniciu, An artificial agent for robust image registration, in: Proceedings of the AAAI conference on artificial intelligence, 31, (1) 2017.

[63] A. Alansary, L.L. Folgoc, G. Vaillant, O. Oktay, Y. Li, W. Bai, J. Passerat-Palmbach, R. Guerrero, K. Kamnitsas, B. Hou, et al., Automatic view planning with multi-scale deep reinforcement learning agents, in: International Conference on Medical Image Computing and Computer-Assisted Intervention, Springer, 2018, pp. 277–285.

[64] J. Ye, Y. Xue, L.R. Long, S. Antani, Z. Xue, K.C. Cheng, X. Huang, Synthetic sample selection via reinforcement learning, in: International Conference on Medical Image Computing and Computer-Assisted Intervention, Springer, 2020, pp. 53–63.

[65] W. Bae, S. Lee, Y. Lee, B. Park, M. Chung, K.-H. Jung, Resource optimized neural architecture search for 3D medical image segmentation, in: International Conference on Medical Image Computing and Computer-Assisted Intervention, Springer, 2019, pp. 228–236.

[66] X. Yang, L. Yu, S. Li, H. Wen, D. Luo, C. Bian, J. Qin, D. Ni, P.-A. Heng, Towards automated semantic segmentation in prenatal volumetric ultrasound, IEEE Trans. Med. Imaging 38 (1) (2018) 180–193.

[67] M. Shalini, S. Radhika, Machine learning techniques for prediction from various breast cancer datasets, in: 2020 Sixth International Conference on Bio Signals, Images, and Instrumentation, ICBSII, IEEE, 2020, pp. 1–5.

[68] J. de Nazaré Silva, A.O. de Carvalho Filho, A. Corrêa Silva, A. Cardoso de Paiva, M. Gattass, Automatic detection of masses in mammograms using quality threshold clustering, correlogram function, and SVM, J. Digit. Imaging 28 (3) (2015) 323–337.

[69] X. Liu, Z. Zeng, A new automatic mass detection method for breast cancer with false positive reduction, Neurocomputing 152 (2015) 388–402.

[70] B. Sanae, A.K. Mounir, F. Youssef, et al., Statistical block-based DWT features for digital mammograms classification, in: 2014 9th International Conference on Intelligent Systems: Theories and Applications (SITA-14), IEEE, 2014, pp. 1–7.

[71] N. Azizi, N. Zemmal, M. Sellami, N. Farah, A new hybrid method combining genetic algorithm and support vector machine classifier: Application to CAD system for mammogram images, in: 2014 International Conference on Multimedia Computing and Systems, ICMCS, IEEE, 2014, pp. 415–420.

[72] F.S.S. de Oliveira, A.O. de Carvalho Filho, A.C. Silva, A.C. de Paiva, M. Gattass, Classification of breast regions as mass and non-mass based on digital mammograms using taxonomic indexes and SVM, Comput. Biol. Med. 57 (2015) 42–53.

[73] A.F. Khalaf, I.A. Yassine, Spectral correlation analysis for microcalcification detection in digital mammogram images, in: 2015 IEEE 12th International Symposium on Biomedical Imaging, ISBI, IEEE, 2015, pp. 88–91.

[74] J. Arevalo, F.A. González, R. Ramos-Pollán, J.L. Oliveira, M.A.G. Lopez, Convolutional neural networks for mammography mass lesion classification, in: 2015 37th Annual International Conference of the IEEE Engineering in Medicine and Biology Society, EMBC, IEEE, 2015, pp. 797–800.

[75] N.S. Ismail, C. Sovuthy, Breast cancer detection based on deep learning technique, in: 2019 International UNIMAS STEM 12th Engineering Conference (EnCon), IEEE, 2019, pp. 89–92.

[76] E.L. Omonigho, M. David, A. Adejo, S. Aliyu, Breast cancer: tumor detection in mammogram images using modified alexnet deep convolution neural network, in: 2020 International Conference in Mathematics, Computer Engineering and Computer Science, ICMCECS, IEEE, 2020, pp. 1–6.

[77] P. Shi, C. Wu, J. Zhong, H. Wang, Deep learning from small dataset for BI-RADS density classification of mammography images, in: 2019 10th International Conference on Information Technology in Medicine and Education, ITME, IEEE, 2019, pp. 102–109.

[78] C. Li, J. Xu, Q. Liu, Y. Zhou, L. Mou, Z. Pu, Y. Xia, H. Zheng, S. Wang, Multi-view mammographic density classification by dilated and attention-guided residual learning, IEEE/ACM Trans. Comput. Biol. Bioinform. 18 (3) (2020) 1003–1013.

[79] M. Alkhaleefah, C.-C. Wu, A hybrid CNN and RBF-based SVM approach for breast cancer classification in mammograms, in: 2018 IEEE International Conference on Systems, Man, and Cybernetics, SMC, IEEE, 2018, pp. 894–899.

[80] A.J. Bekker, H. Greenspan, J. Goldberger, A multi-view deep learning architecture for classification of breast microcalcifications, in: 2016 IEEE 13th International Symposium on Biomedical Imaging, ISBI, IEEE, 2016, pp. 726–730.

[81] M.A. Al-Masni, M.A. Al-Antari, J.-M. Park, G. Gi, T.-Y. Kim, P. Rivera, E. Valarezo, M.-T. Choi, S.-M. Han, T.-S. Kim, Simultaneous detection and classification of breast masses in digital mammograms via a deep learning YOLO-based CAD system, Comput. Methods Programs Biomed. 157 (2018) 85–94.

[82] S.A. Taghanaki, J. Kawahara, B. Miles, G. Hamarneh, Pareto-optimal multi-objective dimensionality reduction deep auto-encoder for mammography classification, Comput. Methods Programs Biomed. 145 (2017) 85–93.

[83] P. Smyth, Bounds on the mean classification error rate of multiple experts, Pattern Recognit. Lett. 17 (12) (1996) 1253–1257.

[84] L. Xu, Least MSE reconstruction: A principle for self-organizing nets, Neural Netw. 6 (627–648) (1993) 22.

[85] M. Kallenberg, K. Petersen, M. Nielsen, A.Y. Ng, P. Diao, C. Igel, C.M. Vachon, K. Holland, R.R. Winkel, N. Karssemeijer, et al., Unsupervised deep learning applied to breast density segmentation and mammographic risk scoring, IEEE Trans. Med. Imaging 35 (5) (2016) 1322–1331.

[86] M. Ranzato, M. Szummer, Semi-supervised learning of compact document representations with deep networks, in: Proceedings of the 25th International Conference on Machine Learning, 2008, pp. 792–799.

[87] S. Guan, M. Loew, Breast cancer detection using synthetic mammograms from generative adversarial networks in convolutional neural networks, J. Med. Imaging 6 (3) (2019) 031411.

[88] J.E. Oliveira, M.O. Gueld, A.d.A. Araújo, B. Ott, T.M. Deserno, Toward a standard reference database for computer-aided mammography, in: Medical Imaging 2008: Computer-Aided Diagnosis, Vol. 6915, SPIE, 2008, pp. 606–614.

[89] J. Suckling, J. Parker, D. Dance, S. Astley, I. Hutt, C. Boggis, I. Ricketts, E. Stamatakis, N. Cerneaz, S. Kok, et al., Mammographic image analysis society (mias) database v1. 21, 2015, URL: https://www.repository.cam.ac.uk/handle/1810/250394.

[90] M. Heath, K. Bowyer, D. Kopans, P. Kegelmeyer, R. Moore, K. Chang, S. Munishkumaran, Current status of the digital database for screening mammography, in: Digital Mammography, Springer, 1998, pp. 457–460.

[91] M.G. Lopez, N. Posada, D.C. Moura, R.R. Pollán, J.M.F. Valiente, C.S. Ortega, M. Solar, G. Diaz-Herrero, I. Ramos, J. Loureiro, et al., BCDR: a breast cancer digital repository, in: 15th International Conference on Experimental Mechanics, Vol. 1215, 2012, pp. 113–120.

[92] I. Moreira, I. Amaral, I. Domingues, A. Cardoso, J.S. Cardoso, INbreast: toward a full-field digital mammographic database, Acad. Radiol. 19 (2) (2012) 236–248.

[93] B.R.N. Matheus, H. Schiabel, Online mammographic images database for development and comparison of CAD schemes, J. Digit. Imaging 24 (3) (2011) 500–506.

[94] A. Bhardwaj, A. Tiwari, Breast cancer diagnosis using genetically optimized neural network model, Expert Syst. Appl. 42 (10) (2015) 4611–4620, http://dx.doi.org/10.1016/j.eswa.2015.01.065.

[95] H.-C. Shin, H.R. Roth, M. Gao, L. Lu, Z. Xu, I. Nogues, J. Yao, D. Mollura, R.M. Summers, Deep convolutional neural networks for computer-aided detection: CNN architectures, dataset characteristics and transfer learning, IEEE Trans. Med. Imaging 35 (5) (2016) 1285–1298, http://dx.doi.org/10.1109/TMI.2016.2528162.

[96] S. Kaymak, A. Helwan, D. Uzun, Breast cancer image classification using artificial neural networks, Procedia Comput. Sci. 120 (2017) 126–131, http://dx.doi.org/10.1016/j.procs.2017.11.219.

[97] J.P. Vink, M. Van Leeuwen, C. Van Deurzen, G. de Haan, Efficient nucleus detector in histopathology images, J. Microsc. 249 (2) (2013) 124–135, http://dx.doi.org/10.1111/jmi.12001.

[98] N. Bayramoglu, J. Kannala, J. Heikkilä, Deep learning for magnification independent breast cancer histopathology image classification, in: 2016 23rd International Conference on Pattern Recognition, ICPR, IEEE, 2016, pp. 2440–2445.

[99] H. Asri, H. Mousannif, H. Al Moatassime, T. Noel, Using machine learning algorithms for breast cancer risk prediction and diagnosis, Procedia Comput. Sci. 83 (2016) 1064–1069.

[100] A. Titoriya, S. Sachdeva, Breast cancer histopathology image classification using AlexNet, in: 2019 4th International Conference on Information Systems and Computer Networks, ISCON, IEEE, 2019, pp. 708–712.

[101] J. Chang, J. Yu, T. Han, H.-j. Chang, E. Park, A method for classifying medical images using transfer learning: A pilot study on histopathology of breast cancer, in: 2017 IEEE 19th International Conference on e-Health Networking, Applications and Services (Healthcom), IEEE, 2017, pp. 1–4.

[102] A.K. Jain, Data clustering: 50 years beyond K-means, Pattern Recognit. Lett. 31 (8) (2010) 651–666.

[103] Y. Wang, B. Lei, A. Elazab, E.-L. Tan, W. Wang, F. Huang, X. Gong, T. Wang, Breast cancer image classification via multi-network features and dual-network orthogonal low-rank learning, IEEE Access 8 (2020) 27779–27792.

[104] L. Roux, D. Racoceanu, F. Capron, J. Calvo, E. Attieh, G. Le Naour, A. Gloaguen, Mitos & Atypia, Tech. Rep 1, Image Pervasive Access Lab (IPAL), Agency Sci., Technol. & Res. Inst. Infocom Res., Singapore, 2014, pp. 1–8.

[105] A. Albayrak, G. Bilgin, Mitosis detection using convolutional neural network based features, in: 2016 IEEE 17th International Symposium on Computational Intelligence and Informatics, CINTI, IEEE, 2016, pp. 000335–000340.

[106] K. Roy, D. Banik, D. Bhattacharjee, M. Nasipuri, Patch-based system for classification of breast histology images using deep learning, Comput. Med. Imaging Graph. 71 (2019) 90–103, http://dx.doi.org/10.1016/j.compmedimag.2018.11.003.

[107] S.M. Patil, L. Tong, M.D. Wang, Generating region of interests for invasive breast cancer in histopathological whole-slide-image, in: 2020 IEEE 44th Annual Computers, Software, and Applications Conference, COMPSAC, IEEE, 2020, pp. 723–728.

[108] J. Xie, R. Liu, J. Luttrell IV, C. Zhang, Deep learning based analysis of histopathological images of breast cancer, Front. Genet. 10 (2019) 80.

[109] A. Das, M.N. Mohanty, P.K. Mallick, P. Tiwari, K. Muhammad, H. Zhu, Breast cancer detection using an ensemble deep learning method, Biomed. Signal Process. Control 70 (2021) 103009.

[110] W.F. Eddy, A new convex hull algorithm for planar sets, ACM Trans. Math. Softw. 3 (4) (1977) 398–403.

[111] L. Van der Maaten, G. Hinton, Visualizing data using t-SNE, J. Mach. Learn. Res. 9 (11) (2008).

[112] F.A. Spanhol, L.S. Oliveira, C. Petitjean, L. Heutte, A dataset for breast cancer histopathological image classification, Ieee Trans. Biomed. Eng. 63 (7) (2015) 1455–1462.

[113] B.E. Bejnordi, M. Veta, P.J. Van Diest, B. Van Ginneken, N. Karssemeijer, G. Litjens, J.A. Van Der Laak, M. Hermsen, Q.F. Manson, M. Balkenhol, et al., Diagnostic assessment of deep learning algorithms for detection of lymph node metastases in women with breast cancer, JAMA 318 (22) (2017) 2199–2210.

[114] E.D. Gelasca, J. Byun, B. Obara, B. Manjunath, Evaluation and benchmark for biological image segmentation, in: 2008 15th IEEE International Conference on Image Processing, IEEE, 2008, pp. 1816–1819.

[115] R.J. Marinelli, K. Montgomery, C.L. Liu, N.H. Shah, W. Prapong, M. Nitzberg, Z.K. Zachariah, G.J. Sherlock, Y. Natkunam, R.B. West, et al., The Stanford tissue microarray database, Nucleic Acids Res. 36 (suppl_1) (2007) D871–D877.

[116] T. Araújo, G. Aresta, E. Castro, J. Rouco, P. Aguiar, C. Eloy, A. Polónia, A. Campilho, Classification of breast cancer histology images using convolutional neural networks, PLoS One 12 (6) (2017) e0177544.

[117] T. Araújo, G. Aresta, C. Eloy, A. Polónia, P. Aguiar, ICIAR 2018 grand challenge on breast cancer histology images, Consortium Open Med. Image Comput. (2017).

[118] M. Lundin, J. Lundin, H. Helin, J. Isola, A digital atlas of breast histopathology: an application of web based virtual microscopy, J. Clin. Pathol. 57 (12) (2004) 1288–1291.

[119] H. Benbrahim, H. Hachimi, A. Amine, Comparative study of machine learning algorithms using the breast cancer dataset, in: International Conference on Advanced Intelligent Systems for Sustainable Development, Springer, 2019, pp. 83–91.

[120] L. Roux, D. Racoceanu, F. Capron, J. Calvo, E. Attieh, G. Le Naour, A. Gloaguen, Mitos & Atypia, Tech. Rep 1, Image Pervasive Access Lab (IPAL), Agency Sci., Technol. & Res. Inst. Infocom Res., Singapore, 2014, pp. 1–8.

[121] O. Ronneberger, P. Fischer, T. Brox, U-net: Convolutional networks for biomedical image segmentation, in: International Conference on Medical Image Computing and Computer-Assisted Intervention, Springer, 2015, pp. 234–241, http://dx.doi.org/10.1007/978-3-319-24574-4_28.

[122] J. Long, E. Shelhamer, T. Darrell, Fully convolutional networks for semantic segmentation, in: Proceedings of the IEEE Conference on Computer Vision and Pattern Recognition, 2015, pp. 3431–3440.

[123] D. Ghosh, A. Kumar, P. Ghosal, T. Chowdhury, A. Sadhu, D. Nandi, Breast lesion segmentation in ultrasound images using deep convolutional neural networks, in: 2020 IEEE Calcutta Conference, CALCON, IEEE, 2020, pp. 318–322, http://dx.doi.org/10.1109/CALCON49167.2020.9106568.

[124] M.H. Yap, G. Pons, J. Mart, S. Ganau, M. Sentis, R. Zwiggelaar, A.K. Davison, R. Marti, Automated breast ultrasound lesions detection using convolutional neural networks, IEEE J. Biomed. Health Inf. 22 (4) (2017) 1218–1226, http://dx.doi.org/10.1109/JBHI.2017.2731873.

[125] G. Latif, M.O. Butt, F.Y. Al Anezi, J. Alghazo, Ultrasound image despeckling and detection of breast cancer using deep CNN, in: 2020 RIVF International Conference on Computing and Communication Technologies, RIVF, IEEE, 2020, pp. 1–5.

[126] K. Wei, B. Wang, J. Saniie, Faster region convolutional neural networks applied to ultrasonic images for breast lesion detection and classification, in: 2020 IEEE International Conference on Electro Information Technology, EIT, IEEE, 2020, pp. 171–174.

[127] S. Ren, K. He, R. Girshick, J. Sun, Faster r-cnn: Towards real-time object detection with region proposal networks, Adv. Neural Inf. Process. Syst. 28 (2015).

[128] C.-Y. Lee, G.-L. Chen, Z.-X. Zhang, Y.-H. Chou, C.-C. Hsu, Is intensity inhomogeneity correction useful for classification of breast cancer in sonograms using deep neural network? J. Healthc. Eng. 2018 (2018).

[129] J.-Z. Cheng, D. Ni, Y.-H. Chou, J. Qin, C.-M. Tiu, Y.-C. Chang, C.-S. Huang, D. Shen, C.-M. Chen, Computer-aided diagnosis with deep learning architecture: applications to breast lesions in US images and pulmonary nodules in CT scans, Sci. Rep. 6 (1) (2016) 1–13, http://dx.doi.org/10.1038/srep24454.

[130] P. Vincent, H. Larochelle, Y. Bengio, P.-A. Manzagol, Extracting and composing robust features with denoising autoencoders, p 1096–1103, in: Proc 25th Int Conf Machine Learn (ICML-08), ACM Press, New York, New York, USA, 2008, pp. 56–60.

[131] P.S. Rodrigues, Breast ultrasound image, Mendeley Data 1 (2017) http://dx.doi.org/10.17632/wmy84gzngw.1, URL: http://dx.doi.org/10.17632/wmy84gzngw.1#file-fa206ab0-b2af453ab8d0-1e6e89230377.

[132] V.S. Parekh, K.J. Macura, S.C. Harvey, I.R. Kamel, R. EI-Khouli, D.A. Bluemke, M.A. Jacobs, Multiparametric deep learning tissue signatures for a radiological biomarker of breast cancer: Preliminary results, Med. Phys. 47 (1) (2020) 75–88, http://dx.doi.org/10.1016/10.1002/mp.13849.

[133] C. Gallego-Ortiz, A.L. Martel, A graph-based lesion characterization and deep embedding approach for improved computer-aided diagnosis of nonmass breast MRI lesions, Med. Image Anal. 51 (2019) 116–124, http://dx.doi.org/10.1016/j.media.2018.10.011.

[134] N. Antropova, B. Huynh, M. Giger, Performance comparison of deep learning and segmentation-based radiomic methods in the task of distinguishing benign and malignant breast lesions on DCE-MRI, in: Medical Imaging 2017: Computer-Aided Diagnosis, Vol. 10134, International Society for Optics and Photonics, 2017, p. 101341G, http://dx.doi.org/10.1117/12.2255582.

[135] H. Zheng, Y. Gu, Y. Qin, X. Huang, J. Yang, G.-Z. Yang, Small lesion classification in dynamic contrast enhancement MRI for breast cancer early detection, in: International Conference on Medical Image Computing and Computer-Assisted Intervention, Springer, 2018, pp. 876–884.

[136] M.U. Dalmış, S. Vreemann, T. Kooi, R.M. Mann, N. Karssemeijer, A. Gubern-Mérida, Fully automated detection of breast cancer in screening MRI using convolutional neural networks, J. Med. Imaging 5 (1) (2018) 014502.

[137] M. Benjelloun, M. El Adoui, M.A. Larhmam, S.A. Mahmoudi, Automated breast tumor segmentation in DCE-MRI using deep learning, in: 2018 4th International Conference on Cloud Computing Technologies and Applications (Cloudtech), IEEE, 2018, pp. 1–6.

[138] A.M. Ibraheem, K.H. Rahouma, H.F. Hamed, Automatic MRI breast tumor detection using discrete wavelet transform and support vector machines, in: 2019 Novel Intelligent and Leading Emerging Sciences Conference, Vol. 1, NILES, IEEE, 2019, pp. 88–91, http://dx.doi.org/10.1109/NILES.2019.8909345.

[139] J. Zhang, A. Saha, Z. Zhu, M.A. Mazurowski, Hierarchical convolutional neural networks for segmentation of breast tumors in MRI with application to radiogenomics, IEEE Trans. Med. Imaging 38 (2) (2018) 435–447, http://dx.doi.org/10.1109/TMI.2018.2865671.

[140] G. Piantadosi, S. Marrone, A. Galli, M. Sansone, C. Sansone, DCE-MRI breast lesions segmentation with a 3TP U-Net deep convolutional neural network, in: 2019 IEEE 32nd International Symposium on Computer-Based Medical Systems, CBMS, IEEE, 2019, pp. 628–633, http://dx.doi.org/10.1109/CBMS.2019.00130.

[141] W. Lu, Z. Wang, Y. He, H. Yu, N. Xiong, J. Wei, Breast cancer detection based on merging four modes MRI using convolutional neural networks, in: ICASSP 2019-2019 IEEE International Conference on Acoustics, Speech and Signal Processing, ICASSP, IEEE, 2019, pp. 1035–1039, http://dx.doi.org/10.1109/ICASSP.2019.8683149.

[142] G. Piantadosi, M. Sansone, C. Sansone, Breast segmentation in MRI via U-Net deep convolutional neural networks, in: 2018 24th International Conference on Pattern Recognition, ICPR, IEEE, 2018, pp. 3917–3922.

[143] X. Xu, L. Fu, Y. Chen, R. Larsson, D. Zhang, S. Suo, J. Hua, J. Zhao, Breast region segmentation being convolutional neural network in dynamic contrast enhanced MRI, in: 2018 40th Annual International Conference of the IEEE Engineering in Medicine and Biology Society, EMBC, IEEE, 2018, pp. 750–753.

[144] G. Piantadosi, M. Sansone, R. Fusco, C. Sansone, Multi-planar 3D breast segmentation in MRI via deep convolutional neural networks, Artif. Intell. Med. 103 (2020) 101781.

[145] F. Bouchebbah, H. Slimani, 3D automatic levels propagation approach to breast MRI tumor segmentation, Expert Syst. Appl. 165 (2021) 113965.

[146] M.U. Dalmış, G. Litjens, K. Holland, A. Setio, R. Mann, N. Karssemeijer, A. Gubern-Mérida, Using deep learning to segment breast and fibroglandular tissue in MRI volumes, Med. Phys. 44 (2) (2017) 533–546, http://dx.doi.org/10.1002/mp.12079.

[147] Y. Nam, G.E. Park, J. Kang, S.H. Kim, Fully automatic assessment of background parenchymal enhancement on breast MRI using machine-learning models, J. Magn. Reson. Imaging 53 (3) (2021) 818–826, http://dx.doi.org/10.1002/jmri.27429.

[148] L. Huo, X. Hu, Q. Xiao, Y. Gu, X. Chu, L. Jiang, Segmentation of whole breast and fibroglandular tissue using nnU-Net in dynamic contrast enhanced MR images, Magn. Reson. Imaging 82 (2021) 31–41, http://dx.doi.org/10.1016/j.mri.2021.06.017.

[149] M. Goto, H. Ito, K. Akazawa, T. Kubota, O. Kizu, K. Yamada, T. Nishimura, Diagnosis of breast tumors by contrast-enhanced MR imaging: Comparison between the diagnostic performance of dynamic enhancement patterns and morphologic features, J. Magn. Reson. Imaging: Off. J. Int. Soc. Magn. Reson. Med. 25 (1) (2007) 104–112.

[150] C.K. Kuhl, H.H. Schild, N. Morakkabati, Dynamic bilateral contrast-enhanced MR imaging of the breast: trade-off between spatial and temporal resolution, Radiology 236 (3) (2005) 789–800.

[151] M.D. Schnall, J. Blume, D.A. Bluemke, G.A. DeAngelis, N. DeBruhl, S. Harms, S.H. Heywang-Kobrunner, N. Hylton, C.K. Kuhl, E.D. Pisano, et al., Diagnostic architectural and dynamic features at breast MR imaging: multicenter study, Radiology 238 (1) (2006) 42–53.

[152] Y. Hiramatsu, C. Muramatsu, H. Kobayashi, T. Hara, H. Fujita, Automated detection of masses on whole breast volume ultrasound scanner: false positive reduction using deep convolutional neural network, in: Medical Imaging 2017: Computer-Aided Diagnosis, Vol. 10134, Spie, 2017, pp. 717–722.

[153] S. Hochreiter, J. Schmidhuber, Long short-term memory, Neural Comput. 9 (8) (1997) 1735–1780, http://dx.doi.org/10.1162/neco.1997.9.8.1735.

[154] C.R. Meyer, T.L. Chenevert, C.J. Galbán, T.D. Johnson, D.A. Hamstra, A. Rehemtulla, B.D. Ross, Data from RIDER-Breast-MRI. The cancer imaging archive, 2015, http://dx.doi.org/10.7937/K9/TCIA.2015.H1SXNUXL.

[155] A. Gallamini, C. Zwarthoed, A. Borra, Positron emission tomography (PET) in oncology, Cancers 6 (4) (2014) 1821–1889, http://dx.doi.org/10.3390/cancers6041821.

[156] A.C. Bourgeois, L.A. Warren, T.T. Chang, S. Embry, K. Hudson, Y.C. Bradley, Role of positron emission tomography/computed tomography in breast cancer, Radiol. Clin. 51 (5) (2013) 781–798, http://dx.doi.org/10.1016/j.rcl.2013.06.003.

[157] S. Hong, J. Li, S. Wang, 18FDG PET-CT for diagnosis of distant metastases in breast cancer patients. a meta-analysis, Surg. Oncol. 22 (2) (2013) 139–143, http://dx.doi.org/10.1016/j.suronc.2013.03.001.

[158] M. Weber, D. Kersting, L. Umutlu, M. Schäfers, C. Rischpler, W.P. Fendler, I. Buvat, K. Herrmann, R. Seifert, Just another "Clever Hans"? Neural networks and FDG PET-CT to predict the outcome of patients with breast cancer, Eur. J. Nucl. Med. Mol. Imaging 48 (10) (2021) 3141–3150, http://dx.doi.org/10.1007/s00259-021-05270-x.

[159] F. Macedo, K. Ladeira, F. Pinho, N. Saraiva, N. Bonito, L. Pinto, F. Gonçalves, Bone metastases: an overview, Oncol. Rev. 11 (1) (2017) http://dx.doi.org/10.4081/oncol.2017.321.

[160] J.H. Choi, H.-A. Kim, W. Kim, I. Lim, I. Lee, B.H. Byun, W.C. Noh, M.-K. Seong, S.-S. Lee, B.I. Kim, et al., Early prediction of neoadjuvant chemotherapy response for advanced breast cancer using PET/MRI image deep learning, Sci. Rep. 10 (1) (2020) 1–11, http://dx.doi.org/10.1038/s41598-020-77875-5.

[161] X. Yang, L. Wu, W. Ye, K. Zhao, Y. Wang, W. Liu, J. Li, H. Li, Z. Liu, C. Liang, Deep learning signature based on staging CT for preoperative prediction of sentinel lymph node metastasis in breast cancer, Acad. Radiol. 27 (9) (2020) 1226–1233, http://dx.doi.org/10.1016/j.acra.2019.11.007.

[162] M. Zarei, A. Rezai, S.S. Falahieh Hamidpour, Breast cancer segmentation based on modified Gaussian mean shift algorithm for infrared thermal images, Comput. Methods Biomech. Biomed. Eng.: Imaging Vis. 9 (6) (2021) 574–580.

[163] P. Kapoor, S. Prasad, Image processing for early diagnosis of breast cancer using infrared images, in: 2010 the 2nd International Conference on Computer and Automation Engineering, ICCAE, vol. 3, IEEE, 2010, pp. 564–566.
[164] S. Kiymet, M.Y. Aslankaya, M. Taskiran, B. Bolat, Breast cancer detection from thermography based on deep neural networks, in: 2019 Innovations in Intelligent Systems and Applications Conference, ASYU, IEEE, 2019, pp. 1–5.
[165] S. Ekici, H. Jawzal, Breast cancer diagnosis using thermography and convolutional neural networks, Med. Hypotheses 137 (2020) 109542.
[166] M.A. Farooq, P. Corcoran, Infrared imaging for human thermography and breast tumor classification using thermal images, in: 2020 31st Irish Signals and Systems Conference, ISSC, IEEE, 2020, pp. 1–6.
[167] G. Zuluaga, Z. Masry, K. Benaggoune, S. Meraghni, A. Noureddine, CNN-based methodology for breast cancer diagnosis using thermal images, 2019, arXiv preprint arXiv:1910.13757.
[168] R. Sánchez-Cauce, J. Pérez-Martín, M. Luque, Multi-input convolutional neural network for breast cancer detection using thermal images and clinical data, Comput. Methods Programs Biomed. 204 (2021) 106045.
[169] S. Chatterjee, S. Biswas, A. Majee, S. Sen, D. Oliva, R. Sarkar, Breast cancer detection from thermal images using a Grunwald-Letnikov-aided Dragonfly algorithm-based deep feature selection method, Comput. Biol. Med. 141 (2022) 105027.
[170] M.A.S. Al Husaini, M.H. Habaebi, T.S. Gunawan, M.R. Islam, E.A. Elsheikh, F. Suliman, Thermal-based early breast cancer detection using inception V3, inception V4 and modified inception MV4, Neural Comput. Appl. 34 (1) (2022) 333–348.
[171] L. Silva, D. Saade, G. Sequeiros, A. Silva, A. Paiva, R. Bravo, A. Conci, A new database for breast research with infrared image, J. Med. Imag. Health Inform. 4 (1) (2014) 92–100, http://dx.doi.org/10.1166/jmihi.2014.1226.
[172] G. Maicas, G. Carneiro, A.P. Bradley, J.C. Nascimento, I. Reid, Deep reinforcement learning for active breast lesion detection from DCE-MRI, in: International Conference on Medical Image Computing and Computer-Assisted Intervention, Springer, 2017, pp. 665–673.
[173] A. Yala, P.G. Mikhael, C. Lehman, G. Lin, F. Strand, Y.-L. Wan, K. Hughes, S. Satuluru, T. Kim, I. Banerjee, et al., Optimizing risk-based breast cancer screening policies with reinforcement learning, Nat. Med. (2022) 1–8.
[174] A. Bhowmik, S. Eskreis-Winkler, Deep learning in breast imaging, BJR| Open 4 (2022) 20210060, http://dx.doi.org/10.1259/bjro.20210060.